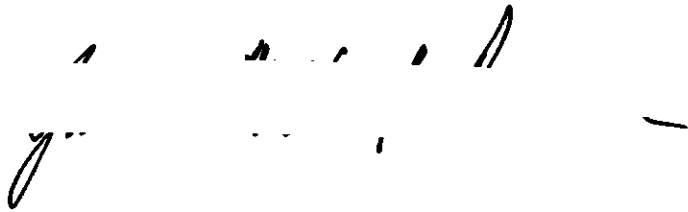


"In presenting the dissertation as a partial fulfillment of the requirements for an advanced degree from the Georgia Institute of Technology, I agree that the Library of the Institution shall make it available for inspection and circulation in accordance with its regulations governing materials of this type. I agree that permission to copy from, or to publish from, this dissertation may be granted by the professor under whose direction it was written, or, in his absence, by the dean of the Graduate Division when such copying or publication is solely for scholarly purposes and does not involve potential financial gain. It is understood that any copying from, or publication of, this dissertation which involves potential financial gain will not be allowed without written permission.



THE INFLUENCE OF DEPTH ON  
THE BEARING CAPACITY OF  
STRIP FOOTINGS IN SAND

A THESIS

Presented to  
The Faculty of the Graduate Division  
by  
James Michael Duncan

In Partial Fulfillment  
of the Requirements for the Degree  
Master of Science in Civil Engineering


Georgia Institute of Technology

March, 1962


12 R

THE INFLUENCE OF DEPTH ON  
THE BEARING CAPACITY OF  
STRIP FOOTINGS IN SAND

Approved:

  
Aleksandar B. Vesic

  
George F. Sowers

  
R. K. Jacobs

Date approved by chairman: Jan. 8, 1962

## ACKNOWLEDGMENTS

The writer wishes to express his deep appreciation to Professor Dr. Aleksandar B. Vesic for his suggestion of this research and his guidance during its execution. Gratitude is extended to Professors George F. Sowers and R. K. Jacobs for their helpful comments on the text.

To my wife, Annella, I wish to extend my thanks for her aid in preparation of the manuscript.

## TABLE OF CONTENTS

|  | Page |
|--|------|
| ACKNOWLEDGMENTS . . . . .                  | ii   |
| LIST OF TABLES . . . . .                   | iv   |
| LIST OF ILLUSTRATIONS . . . . .            | v    |
| SUMMARY . . . . .                          | vi   |
| CHAPTER                                    |      |
| I.    INTRODUCTION . . . . .               | 1    |
| II.   EQUIPMENT AND PROCEDURE . . . . .    | 8    |
| III.  DISCUSSION OF TEST RESULTS . . . . . | 24   |
| IV.   CONCLUSIONS . . . . .                | 45   |
| V.    RECOMMENDATIONS . . . . .            | 46   |
| APPENDIX . . . . .                         | 47   |
| NOTATIONS . . . . .                        | 48   |
| TABLES . . . . .                           | 50   |
| BIBLIOGRAPHY . . . . .                     | 68   |

## LIST OF TABLES

| Table |  | Page |
|-------|--|------|
| 1.    | Summary of Significant Results from Footing Load Tests . .   | 31   |
| 2.    | Average $N_q$ Values . . . . .                               | 34   |
| 3.    | Angle of Friction $\phi_E$ Deduced from Load Tests . . . . . | 36   |
| 4.    | Summary of Results from Skin Load Tests . . . . .            | 40   |
| 5.    | Point Load Settlement Data . . . . .                         | 50   |
| 6.    | Skin Load Settlement Data . . . . .                          | 60   |

## LIST OF ILLUSTRATIONS

| Figure |   | Page |
|--------|---|------|
| 1.     | Shallow and Deep Foundations and Rupture Figures . . . .  | 2    |
| 2.     | Sketches of Equipment . . . . .   | 9    |
| 3.     | Density of Sand as a Function of Height of Fall . . . .   | 11   |
| 4.     | Penetrometer Resistance as a Function of Depth for<br>Several Densities . . . . .                       | 19   |
| 5.     | Grain-size Distribution Curve . . . . .   | 20   |
| 6.     | Angle of Internal Friction as a Function of Void Ratio .  | 21   |
| 7.     | Initial Tangent Modulus of Deformation as a Function of<br>the Ratio $\sigma_1/\sigma_3$ . . . . .      | 22   |
| 8.     | Initial Tangent Modulus of Deformation as a Function<br>of $\sigma_3$ . . . . .                         | 23   |
| 9.     | Load Settlement Curves . . . . .  | 26   |
| 10.    | Photographs. a. General Shear Failure. b. An Unbraced<br>Cut in the Sand. . . . .                       | 27   |
| 11.    | Comparison of Theoretical and Experimental Bearing<br>Capacity Factor . . . . .                         | 28   |
| 12.    | a. Cohesion as a Function of Void Ratio. b. Contribu-<br>tion of Cohesion to Bearing Capacity . . . . . | 29   |
| 13.    | Ultimate Bearing Capacity as a Function of Depth . . . .  | 33   |
| 14.    | Ratio $\phi_E/\phi$ as a Function of Relative Density . . . . .   | 37   |
| 15.    | Comparison of Ultimate Bearing Capacity and Penetration<br>Resistance . . . . .                         | 39   |
| 16.    | $E/1 - v^2$ as a Function of Depth . . . . .  | 44   |

## SUMMARY

The purpose of this investigation was to establish the relationship between footing depth and bearing capacity for a medium uniform sand. This purpose was accomplished by load tests of 2 inch by 12 inch footings at the surface and buried at 4 depths in sand placed at four different densities. The footings were arranged so that the base and the lateral surface could be loaded separately, and the magnitude of point and skin resistance examined separately. Checks of density and homogeneity were made by soundings with a small penetrometer.

These tests show that for a footing buried in a relatively homogeneous mass of sand, bearing capacity increases with depth at a constantly decreasing rate. Since all theories so far presented predict a linear increase of bearing capacity with depth, even those which predict the lowest bearing capacities are unconservative after some depth.

The resistance to penetration by a small penetrometer is from two to four times as great as bearing capacity (defined by some limiting settlement) of a footing in the same mass of sand, the difference increasing with depth and with the density of the sand.

Measured values of average skin friction seem to be fairly constant for sand which is placed by the same method, regardless of density. Skin friction for models built by dropping the sand into place is about 55 per cent of skin friction for models built compacting the sand by vibration.



Pulling tests for determination of skin friction indicate that for compacted sands, the skin friction which acts during the initial downward loading may be more than twice as great as that which acts when the foundation is pulled upward.

Valuable extensions of this study can be made by determination of the effect of the absolute size of the footing and penetrometers used, and separation of the effects of changes in angle of internal friction and changes in relative density. Also qualitative tests to discover the phenomenon of foundation failure would contribute greatly to a solution of the problem.

## CHAPTER I

## INTRODUCTION

The practical problem of computing the bearing capacity of a real foundation is usually idealized as shown in Fig. 1a (shallow) and Fig. 1c (deep). The shallow foundation is treated as a loaded strip at the surface of a semiinfinite mass. The properties of this mass are assumed to be completely described by the constants  $c$ ,  $\phi$ , and  $\gamma$  (see Appendix). Further it is assumed that the strength of the mass can be expressed by Coulomb's equation for failure;

$$\tau = c + \bar{\sigma} \tan \phi$$

and that the mass behaves as a rigid-plastic material. No consideration is given to strain before failure, so that the problem of ultimate bearing capacity is treated separately from that of settlement.

The surface outside the loaded strip may be loaded with a surcharge,  $q$ .

Prandtl solved this problem for the special case of soil without weight ( $\gamma = 0$ ). The solution is of the form

$$q_{ult} = cN_c + qN_q$$

where  $N_c$  and  $N_q$  are dimensionless bearing capacity factors and are functions of  $\phi$  only. Terzaghi solved another special case for cohesionless soil ( $c = 0$ ) with weight ( $\gamma \neq 0$ ). When  $q = 0$  the solution takes the form

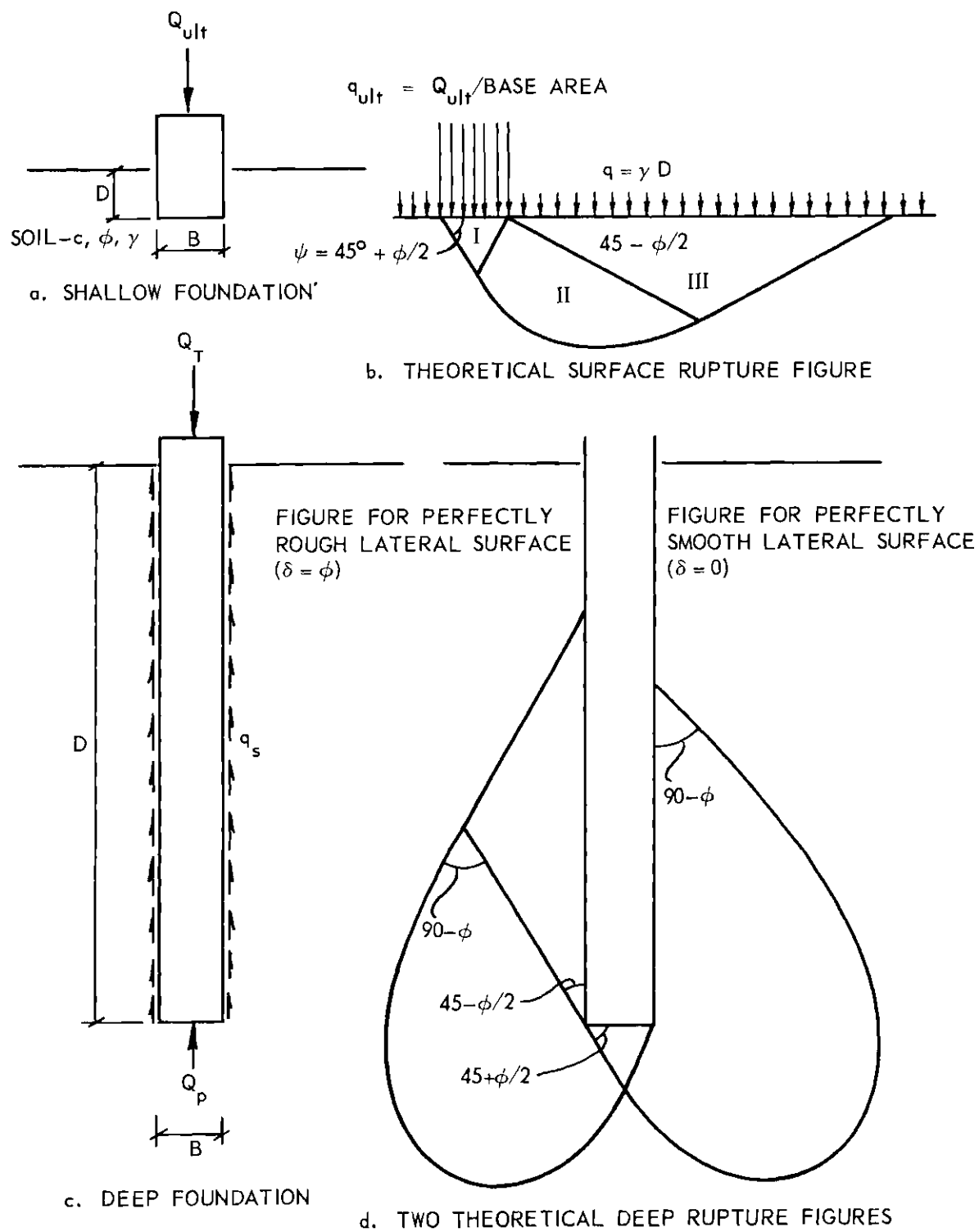


Figure 1. Shallow and Deep Foundations and Rupture Figures.

$$q_{ult} = \frac{1}{2}\gamma B N_\gamma$$

where  $N_\gamma$  is also a dimensionless factor which is a function of  $\phi$  only.

Since a closed solution of the general case ( $c \neq 0$ ,  $\gamma \neq 0$ ) has not yet been made, it has been suggested by Terzaghi (1) and others that for the general case the special cases can be added so that the solution takes the form

$$q_{ult} = cN_c + qN_q + \frac{1}{2}\gamma B N_\gamma$$

At failure three distinct zones form under the foundation, as shown in Fig. 1b. Zone I is a dense elastic zone which moves down with the foundation, zone II is a zone of radial shear (Prandtl zone) which moves generally horizontally, and zone III is a passive Rankine zone which moves up. Prandtl's solution gave for the angle  $\psi$ , Fig. 1b,  $45 + \phi/2$ . Terzaghi assumed that this would be the case only for a perfectly smooth base, because any roughness would make it possible for the major principal stress,  $\sigma_1$ , to be non-vertical, thus reducing the extent of the elastic wedge and the shear zones and reducing the bearing capacity.

De Beer and Vesic (2) have shown by model tests at the surface that: (1) the phenomenon is as theory predicts for dense sands ( $R_D \geq 0.67$ ), (2) the angle  $\psi$  is always greater than or equal to  $45 + \phi/2$ , and (3) this theory gives values of  $N_\gamma$  which show close agreement with the experimental, as determined by tests on model footings which varied in width up to 3".

The problem of determination of the ultimate bearing capacity of a deep foundation is usually separated into two parts: determination of

point resistance and lateral or skin resistance. The total bearing capacity,  $Q_t$ , is usually expressed as

$$Q_t = Q_p + Q_s$$

where  $Q_p$  = point resistance and  $Q_s$  = skin resistance.

Skin resistance is usually rationally computed. Some average skin resistance  $q_s$  is computed so that

$$Q_s = q_s A_s$$

In the general case of deep foundations in materials with both cohesion and internal friction,  $q_s$  is composed of an adhesion term and a friction term.

$$q_s = mc + \frac{1}{2}\gamma D K_s \tan \delta$$

where  $m$  is a dimensionless constant less than or equal to one; expressed as a ratio,  $m$  = adhesion/cohesion. The above formula assumes that the adhesion term is constant over the lateral surface and that the friction term varies linearly with vertical pressure. The tangent of the skin friction angle,  $\delta$ , is usually assumed to be some constant,  $\alpha$ , times tangent  $\phi$ . The value of  $\alpha$  depends on the roughness of the lateral surface of the foundation and is always less than or equal to one.

We may now express the unit skin resistance as

$$q_s = \frac{1}{2}\gamma D K_s \alpha \tan \phi$$

for foundations in cohesionless materials. Although  $Q_s$  may be a large

part of  $Q_t$  in the case of a deep foundation in a cohesive material, it is usually only 10 per cent to 20 per cent of  $Q_t$  for deep foundations in cohesionless materials. That  $Q_s$  is small in the ordinary case may be seen from the values of  $q_p$  and  $q_s$  given in Tables 5 and 6, respectively. Because it is small it is usually of only secondary importance, and the problem of determining point resistance is the main one in materials with no cohesion.

The ultimate point load,  $Q_p$ , can be expressed by

$$Q_p = A_p q_{ult}$$

where  $q_{ult}$  is the average ultimate pressure which may develop on the point. The results of most theories which have been advanced can be expressed in the form

$$q_{ult} = cN_c + \gamma D N_q + \frac{1}{2}\gamma B N_\gamma$$

$N_c$ ,  $N_q$ , and  $N_\gamma$  are dimensionless factors and are all of the same order of magnitude. Because  $B$  is small compared to  $D$  for deep foundations, the term  $\frac{1}{2}\gamma B N_\gamma$  is usually neglected and  $q_{ult}$  is given by

$$q_{ult} = cN_c + \gamma D N_q$$

Coulomb's equation for the failure envelope

$$\tau = c + \bar{\sigma} \tan \phi$$

may also be written

$$\tau = (c \cot \phi + \bar{\sigma}) \tan \phi$$

$N_c$  may be derived from  $N_q$  by use of this fact, and is found to be  
 $N_c = (N_q - 1) \cot \phi$ . Thus the determination of  $N_q$  is the only problem.

The bearing capacity theory for shallow foundations may be used directly for deep foundations if it is assumed that the soil above the level of the base acts only as a surcharge,  $q = \gamma D$ . This method does not take into account any of the properties of that part of the mass above the base except the weight.

There are several theories which attempt to take into account the strength of the soil around the foundation as well as below its base (3). These theories usually assume some general shape for a figure of rupture and then determine the position and size for this figure which makes the ultimate pressure a minimum. Fig. 1d shows two such rupture figures.

One theory which has been advanced is different from the others in that it assumes no rupture figure, but instead that the ultimate pressure is the same as that required to expand a sphere inside the material with its center at the same level as the base of the foundation. This is an extension to materials with internal friction of a theory by Bishop, Hill and Mott (4) concerning the resistance to punching metals. This approach in its original form was used for determination of bearing capacity of deep foundations in frictionless materials and gave results which agree with experiments as well as other theories.

The theories so far presented differ somewhat in assumptions and values of  $N_q$ . They give values of  $N_q$  which vary from 50 to 150 for  $\phi = 30^\circ$  and from 190 to 1000 for  $\phi = 40^\circ$ . They all give a constant value of  $N_q$ , at least after some minimum depth (enough to contain the full rupture figure). That is to say, they all predict a linear increase of bearing capacity with depth for depths over some minimum value.

The purpose of this investigation was to establish the relationship between footing depth and bearing capacity for a medium uniform sand. This was accomplished by load tests of model footings buried at various depths in sand placed at different densities.

The soil mechanics literature contains a great number of reports of load tests performed in the field on full scale piles. Although load tests at the site may be the single most valuable aid to design of a pile foundation, such tests contribute little toward formulation of a theory of bearing capacity. Two things usually seriously reduce the value of field tests for comparison with theory: (1) when load tests are made, they are not often preceded by extensive subsoil investigation, and (2) foundations which are load-tested are usually driven piles; they present complex conditions and must be considered under more complicated theories.

Load tests of deep foundations under controlled, well known conditions are relatively few. Valuable contributions have recently been made for cohesive soils (5) and for sands (6) also. Many questions, both quantitative and qualitative, about the actual physical behavior of deep foundations still remain unanswered.

Load tests under refined conditions which approach the theoretical conditions serve both as a quantitative check on the practical results of existing theories and may provide clues to development of new theories.



## CHAPTER II

### EQUIPMENT AND PROCEDURE

#### Construction of Models

As used here, model means both the footing which was buried and the sand in which it was buried. Construction consists of placing both the sand and the footing. In building these models, every effort was made to keep them as homogeneous as possible with respect to density. The technique used to achieve this homogeneity was to drop the sand into place from a definite height. For any given set of equipment an empirical relationship may be established between height of free fall of the sand and the density corresponding.

#### Equipment

In order to use this technique the following equipment is necessary: (1) a dry sand, (2) a box in which to deposit the sand, (3) a device (described here as a funnel) from which the sand can be discharged, with zero initial velocity, in a uniform pattern over the desired area, (4) an elevated reservoir of sand from which the funnel can be supplied, (5) a means of adjusting the height of fall of the sand.

The box in which the models were constructed was steel, 50 inches square, 70 inches deep, see Fig. 2. One side of the box had two doors, one above the other, to facilitate emptying. The funnels used were developed by trial and error. Those eventually used were 6 inches wide, and 13 inches and 23 inches in length. From rectangular bottoms of the

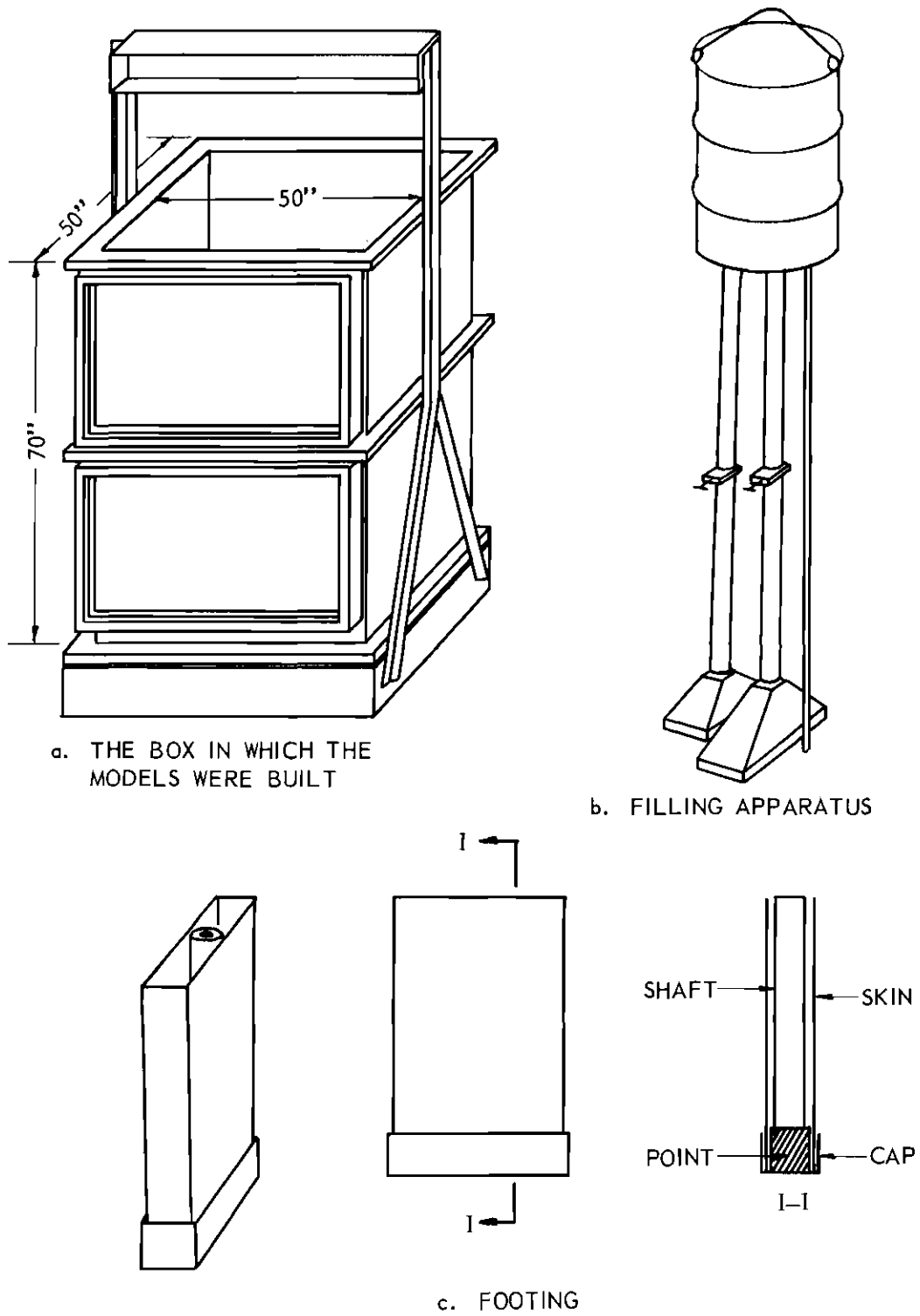


Figure 2. Sketches of Equipment.

dimensions given they tapered up, pyramid-like, for 12 inches to  $2\frac{1}{2}$  inch rubber hoses. These hoses were nine feet long and connected to a 55 gallon drum at their upper end. At mid-height each had a valve for regulating the flow of sand to the funnels. The bottom of the funnels was a piece of perforated hardboard, with  $\frac{3}{16}$  inch diameter holes on  $\frac{1}{2}$  inch square centers. This pattern gives 11 per cent open area. To keep the surface smooth for the intermediate heights of fall, the rate of flow was decreased by closing half of the holes (every other line) with masking tape. The full open area was used for the  $\frac{1}{2}$  inch height of fall and for placing the sand prior to vibration to achieve the most dense state in order to save time.

Calibration.--Before any models were built, the relationship of height of fall and resulting density was established. The result of this calibration is shown in Fig. 3. A shallow box (12" deep) of approximately half the area (24" by 48") of the box in which the models were constructed was used for this calibration. This box was placed on a 1600 lb. capacity scale and filled using the same procedure used in building the models. In the first trials the box was not filled completely. This procedure gave a greater scattering of the points attained than filling the box completely, because of the difficulty of estimating the volume which had been filled. The calibration was completed by overfilling the box and cutting the surface of the sand level with the top. A box of this size was used in order to approximate the conditions under which the models were built. The curve shown in Fig. 3 applies only when there is relatively free flow of air around and through the falling sand. The density

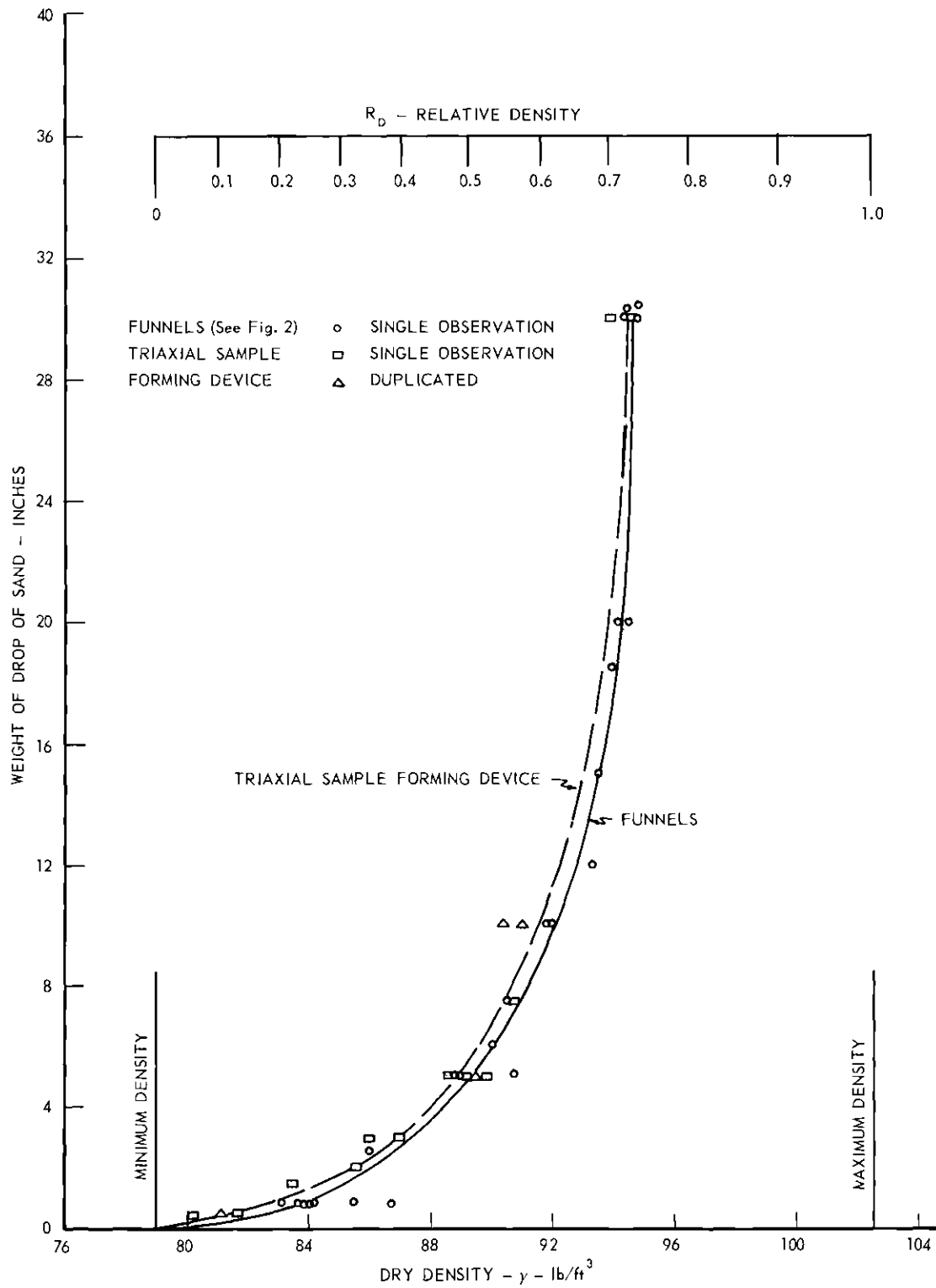


Figure 3. Density of Sand as a Function of Height of Fall.

achieved is a direct function (empirically a log function) of the energy expended in compaction. Compactive effort increases, however, only so long as the velocity and thus the kinetic energy increases with height of fall. There is a terminal velocity of sand falling freely through air, and this velocity is decreased very appreciably by restriction of air flow around the falling sand. Some observations, by the author, in forming triaxial samples by the same method indicate that when air flow is severely restricted the maximum density obtainable at any height of fall is of the order  $R_D = 0.3$ .

Similarly, checks were made in the laboratory of the effectiveness of vibration before any models were built by this method. The variables are many: vibrator power, vibrator frequency, plate thickness, time of vibration, additional surcharge, layer thickness and density before vibration. Although this is an extremely complicated problem, most of these factors were set arbitrarily and only layer thickness and time of vibration varied until a convenient method was found which yielded a high degree of compaction,  $R_D = 0.9$ . The sand was deposited in a four inch layer, with no adjustment of height, from an average height of 30". The sand was subjected to vibration at its surface for three minutes. Two electric vibrators were used; input power 275 watts each, frequency 3600 cycles per minute. Although amplitude is variable on these vibrators, maximum amplitude, about  $1/32$  inch, was used at all times in order to have maximum acceleration (7). The vibrators were attached at the centers of two  $\frac{1}{4}$  inch steel plates 24 inches by 48 inches.

### Method of Construction

The filling procedure was as follows. For  $\frac{1}{2}$  inch (average) height of fall: the barrel, with hoses attached to its under side was lifted into position over the box and its height adjusted so that the funnels hung one inch from the surface of the sand already deposited. The six inch by 13 inch funnel was held in one corner of the box and the valve opened, allowing sand to run into the funnel, and from the funnel into the box. This position was held until sand had filled up to the bottom of the funnel, stopped flow from the funnel, and the funnel and hose above it were full of sand. Then the valve was closed and the funnel moved slowly along the side of the box perpendicular to the long side of the funnel, allowing sand to fill the entire one inch before the funnel was moved on. In this way two strips of sand 13 inches wide were deposited on opposite sides of the box. Then, with the 6 inch by 23 inch funnel, a strip was laid down in the center of the box, between those previously deposited. The unfilled areas (which had the appearance of valleys), always present at the edge of the box, were filled with a  $\frac{3}{4}$  inch hose which had a valve at its end. No attempt was made to keep this sand at the same density, since it was at the sides of the box and its character probably quite unimportant to the quality of the model. After each one inch layer was deposited, the barrel was raised one inch and the process repeated. Those footings whose bases were below the surface were buried; that is, the sand was deposited around them after they had been fixed carefully in place with their bases in contact with the sand beneath. Construction above the bases of the footings was done by depositing the sand from the 6 inch by 23 inch funnel only in two

strips, one on either side of the footing. Both immediately beneath the footings and at the top of the box the sand was cut to a level surface with a thin piece of metal sharpened on one edge. When the box was filled to the required height the frame which had supported the footings was removed and the loading and deflection measuring equipment was set in place.

For 6 inch and 30 inch (average) heights of fall a similar procedure was used, with the exception that the funnels were moved back and forth over the surface beginning immediately when the valve was opened. The funnel heights were set at  $6\frac{1}{2}$  inches for the 6 inch drop and a one inch layer was deposited; at 31 inches for the 30 inch drop and a two inch layer was deposited (since at greater heights density is relatively insensitive to small changes in height). For the vibrated density the sand was deposited in a four inch layer, with no adjustment of height, from an average height of 30 inches. Then the sand was subjected to vibration at its surface for three minutes. During vibration the plates were moved from side to side, always butting against one another to prevent formation of a less dense area at their junction. On one side these plates had a removable plug  $\frac{1}{4}$  inch larger than one half of the footing. Above the base of the footing they were placed around the footing and vibration was done as before, except that the plates were held still and not allowed to touch the footing.

#### Load Tests

##### Footings

Two different types of footing were used in these tests. For surface tests a 2 inch by 12 inch aluminum plate  $\frac{1}{2}$  inch thick was used.

For tests beneath the surface, steel footings, shown in Fig. 2, were used. These footings were built with a telescoping arrangement so that the point could be pushed first, separate from the skin, then the skin could be pushed separately, then both as a unit. The first three ten-inch deep tests were made without the cap, but with this arrangement sand flowed between the point and the skin during the loading of the skin causing high mechanical friction. This mechanical friction was larger than the skin friction which was being measured. To overcome this the cap was added, changing the point from 2 inches by 12 inches to 2.44 inches by 12.44 inches. This reduced the mechanical friction to a very small amount.

#### Loading Procedure

For surface tests two different loading devices were used. Tests 1, 2, and 3 were made using an aluminum beam with a small screw jack for application of load. This beam was quite flexible, and near the end of tests 1 and 2 it had approximately a  $3/4$  inch bow in it. This is of interest and importance because it changed the character of load application. If a very rigid beam is used for the jack reaction, load application is essentially strain controlled although the load is applied in increments of stress. This is because if the footing deflects a very small amount, the stress is reduced appreciably; that is, the footing can "run away" from the load by deflecting a very small amount. On the other hand, if the loading beam deflects a large amount a small deflection of the footing will not appreciably reduce the load, and the loading is more nearly stress- than strain-controlled. This was very obvious at the end of the tests 1 and 2 when the footings jumped into the sand at ultimate load.



No such jump could have occurred with the screw jack used, if the loading beam had been rigid. A hydraulic jack attached to the rigid load frame was used for the other surface test, 16. For all surface tests the footing was attached rigidly to the bottom of the proving ring used to measure load. This proving ring was attached to the bottom of the jack. With this arrangement loading could start from zero pressure because the footing was initially suspended from the proving ring rather than resting on the sand. Two dial gages were used to measure settlement, one on either side of the proving ring. Two gages serve as a check on each other as well as indicating any tilt in the footing. An average of the separate gage readings was taken for axial settlement. Load was applied in increments of  $1/15$  of the estimated ultimate load at one minute intervals. Settlement dials were read immediately before the next load increment was applied.

For tests beneath the surface three separate loadings were made. First, with the skin clamped in position, the point was loaded using the same procedure as for a surface test. In all deep tests a hydraulic jack connected to the rigid loading frame was used for load application. After the point had been loaded, the skin was unclamped and it was loaded in increments of  $1/10$  of the estimated ultimate load. It was pushed until it had settled the same amount and returned to its original position relative to the point. Deflection and load were measured in the same way as for surface tests and deep point load. After the skin was loaded both point and skin were loaded as a unit. The main purpose of this loading was to check that the load required was approximately equal to the loads required to push the point and skin separately.

### Penetrometer Soundings

In order to check the homogeneity of each model, at least two penetrometer soundings were made in each model after the load test. The penetrometer used was  $1/2$  inch in diameter at the point and had a  $3/8$  inch diameter skin. It was built on the same telescoping principle as the footings. These soundings were static, rather than dynamic. The penetrometer was pushed by a screw-jack at about four inches per minute. The result of the soundings is a graph of penetrometer resistance vs. depth. Because of the fact that the skin of the penetrometer was  $1/8$  inch smaller than the point, and because there was always mechanical friction between point and skin, skin friction measurements were not consistent, and are not believed to be accurate. However, because the force required to push the point was always about 90 to 95 per cent of the force required to push point and skin together, total resistance plotted as pressure on the point is very near the true point resistance. When used this way, the soundings are more consistent and valuable.

As will be shown later, there is no bearing capacity theory which will give the density as a function of point resistance, even when the relation between density and angle of internal friction has been established. For this reason, it was necessary to establish this relationship empirically by a controlled calibration. A box 24 inches wide, 16 inches long and 60 inches deep was placed on a 1600 pound capacity scale and filled by the same method as used for building the models. The same care was exercised to keep the sand homogeneous with respect to density. When the box had been filled and the average density checked, two penetrometer soundings were made in this box using the same method as for

sounding in the models. The results of these tests are curves of penetrometer resistance vs. depth for various average densities, Fig. 4. Using these curves an estimate of the density of the load-test models in the vicinity of the point can be made. Further comments on the results of this calibration and the penetrometer soundings will be made in Chapter III.

#### Physical Properties of the Sand

The sand used in building these models was a medium, uniform, subangular micaceous Chattahoochee River sand. It was air dried and sieved through a window screen (about equivalent to a standard number 16 sieve). A grain-size curve is shown in Fig. 5. Minimum density was 79.0 lb/ft<sup>3</sup>, maximum density was 102.5 lb/ft<sup>3</sup>. Normal triaxial tests (compression tests with  $\sigma_3$  constant) were made for this sand at densities of 84, 90, 95, and 98 lb/ft<sup>3</sup>. Lateral pressures of 5, 10, 20, 40, and 80 lb/in<sup>2</sup> were used for each density. The result of these tests is the curve shown in Fig. 6, giving the angle of internal friction as a function of the void ratio,  $e$ . Also some triaxial tests were made in which the ratio  $\sigma_1/\sigma_3$  was kept at a constant value while  $\sigma_1$  was increased. Tests were made for the same four densities and ratios  $\sigma_1/\sigma_3$  of 1.5, 2.0, 3.0, and 4.0. Not all of these ratios could be used for the less dense samples, because they failed immediately when the test began. The main value of these tests is in determining the modulus of deformation,  $E$ , as a function of density and lateral pressure ratio. Curves showing tangent modulus of deformation,  $E_t$ , as a function of the ratio  $\sigma_1/\sigma_3 = k$  are given in Fig. 7.  $E_t$  from the normal triaxial tests as a function of  $\sigma_3$  is given in Fig. 8.

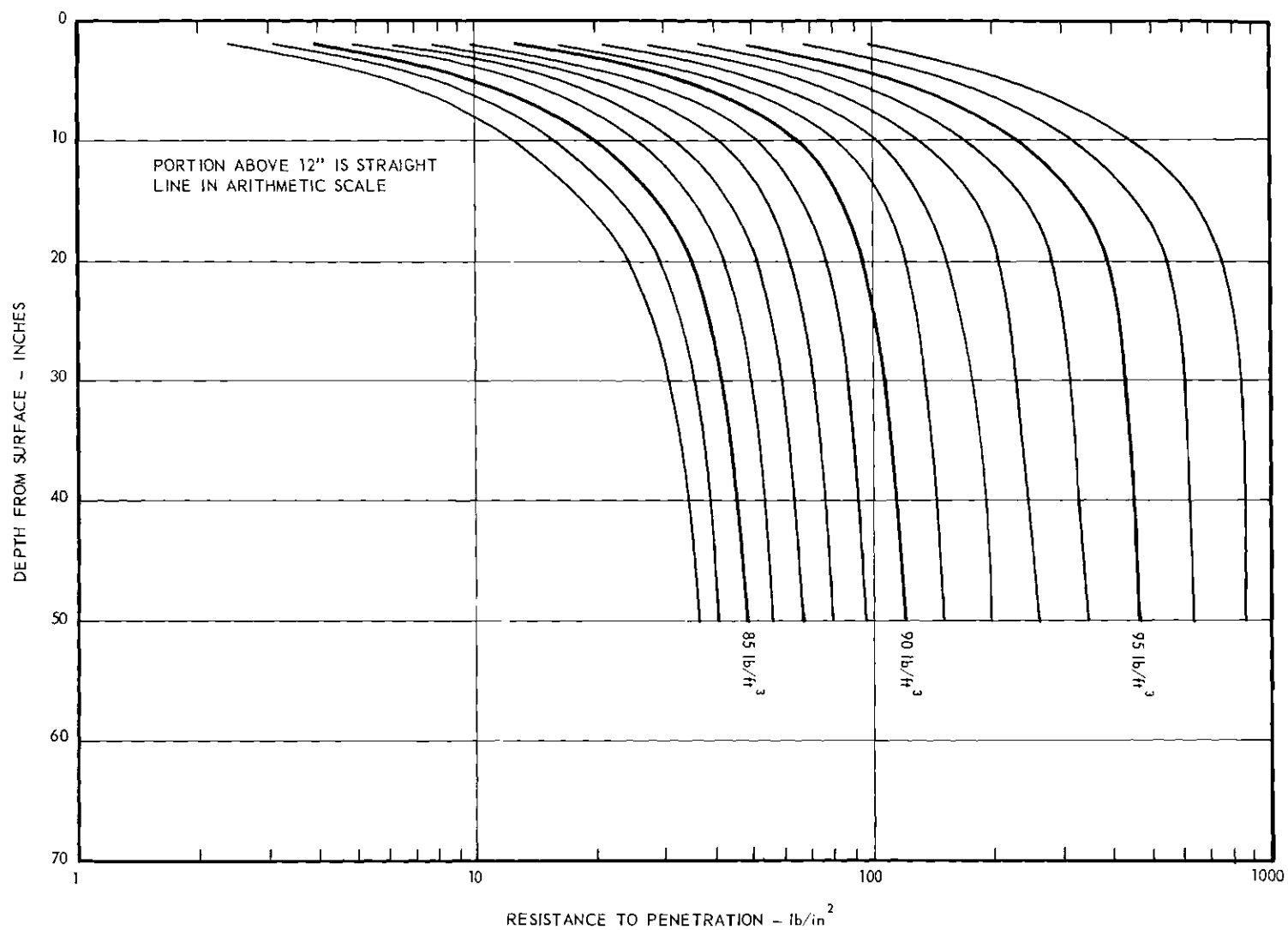


Figure 4. Pentrometer Resistance as a Function of Depth for Several Densities.

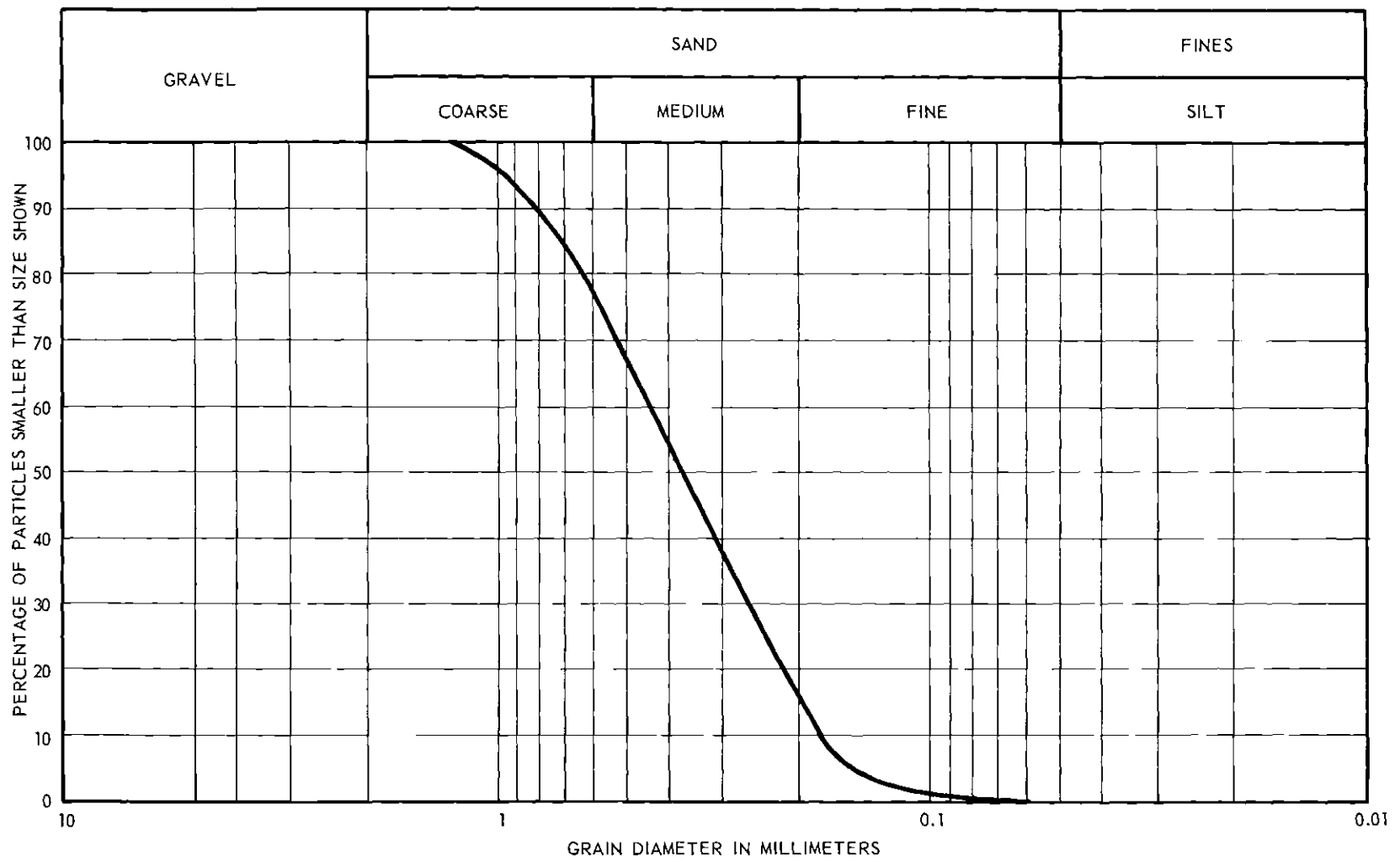


Figure 5. Grain-size Distribution Curve.

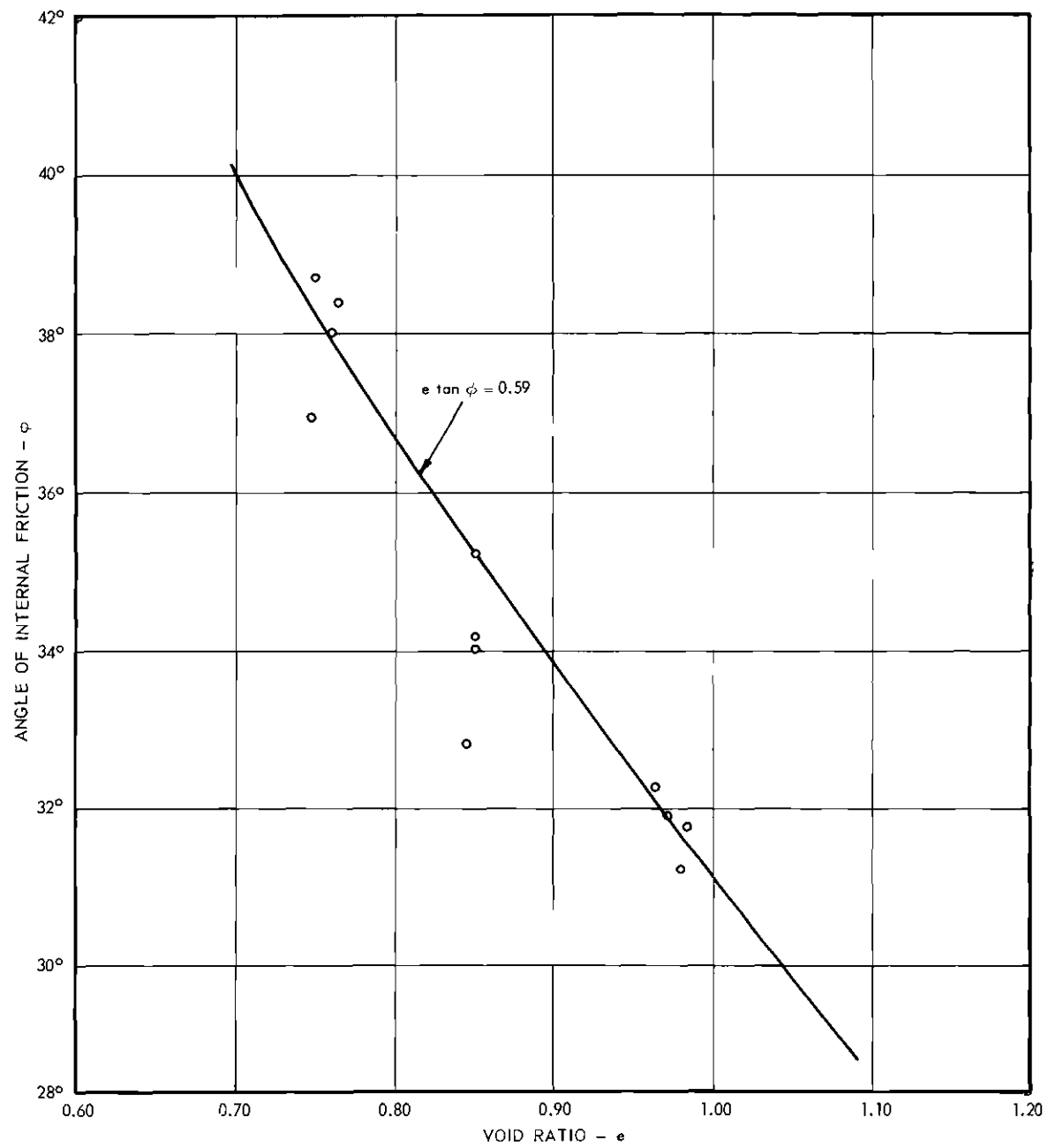


Figure 6. Angle of Internal Friction as a Function of Void Ratio.

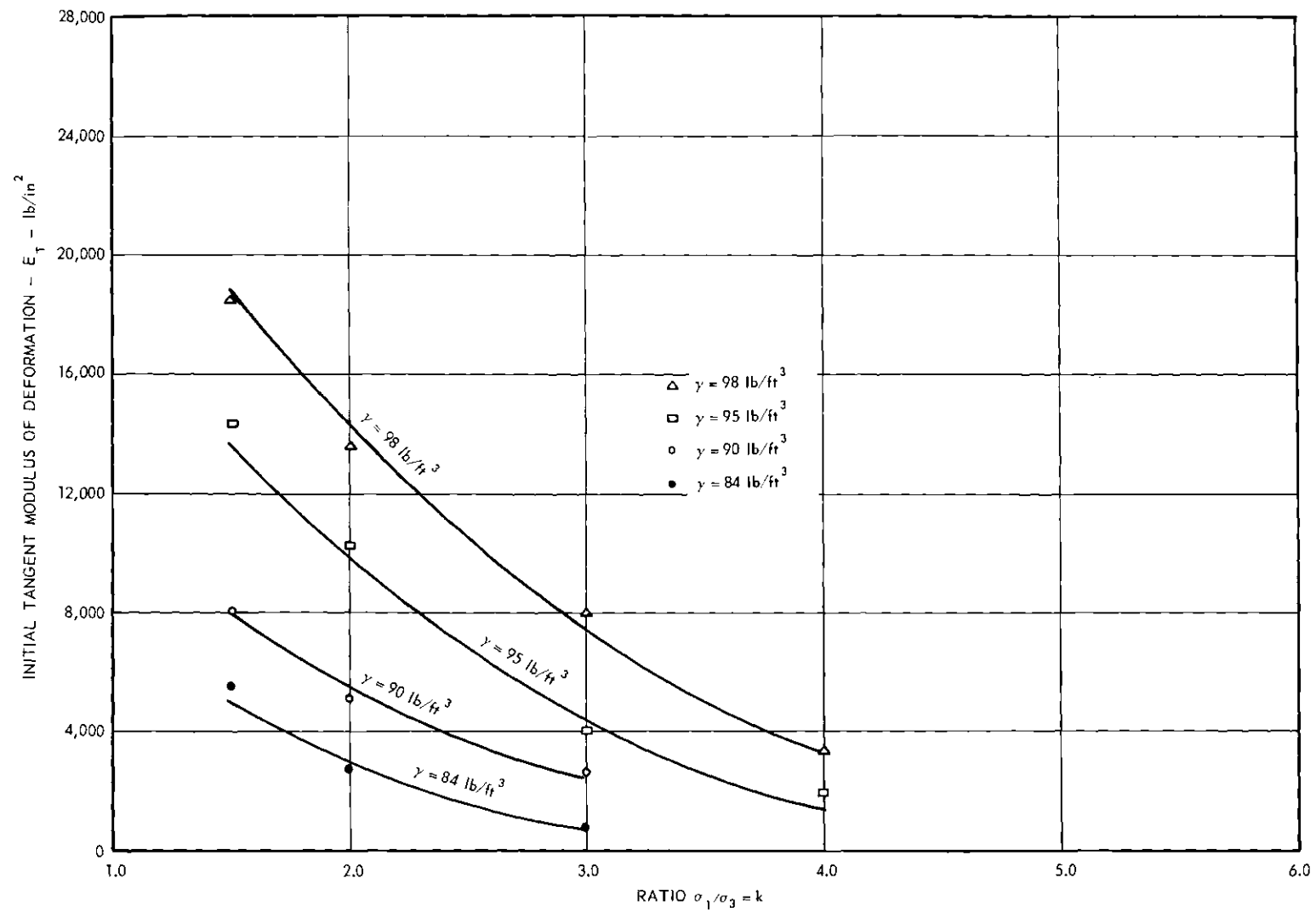


Figure 7. Initial Tangent Modulus of Deformation as a Function of the Ratio  $\sigma_1/\sigma_3$ .

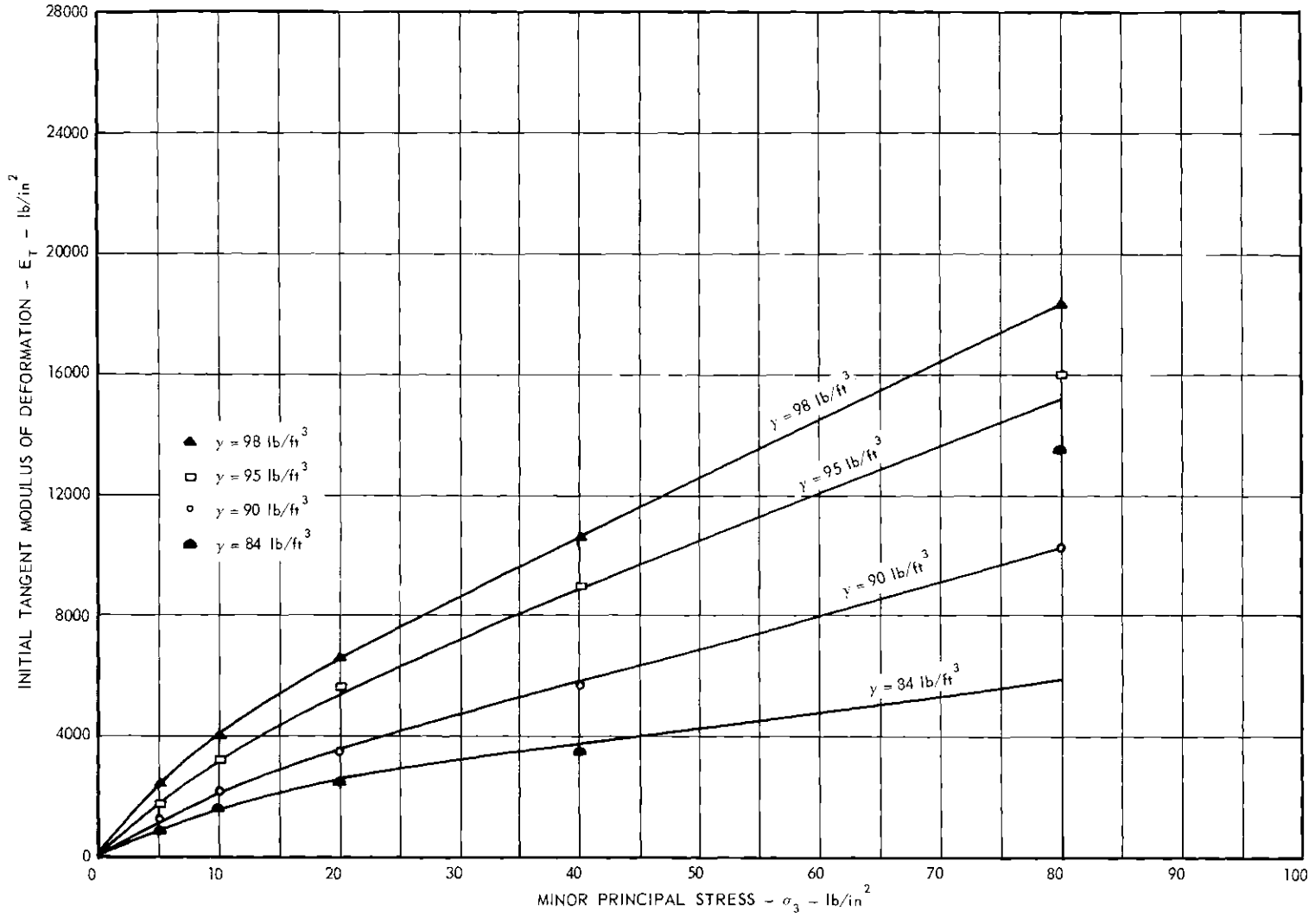


Figure 8. Initial Tangent Modulus as a Function of  $\sigma_3$ .



## CHAPTER III

## DISCUSSION OF RESULTS

The first step in analyzing these data was to establish a failure or ultimate load criterion. In those cases where load reaches a true maximum and drops off or remains constant with increased settlement this is not difficult. But for all tests below a depth of 20 inches and for all tests where the sand was at relative density 0.5 or less, no apparent maximum was reached. In order to simplify the analysis and make the results of the tests consistent, the following criterion was adopted (8): ultimate pressure was taken as the pressure which corresponded to the amount of settlement at which the most dense model, at the same depth, failed. Although this is not true failure, adoption of some such criterion is necessitated by the fact that all but the most dense sands are compressible, and very great strains occur with no failure. The adoption of this criterion reduced the problem to determination of ultimate pressure for only the most dense models. At depths of 0, 10, and 20 inches at the highest density a true maximum pressure was reached. At the depths of 30 and 40 inches, however, a sharp increase in the rate of settlement (similar to yield of a ductile metal) was taken as failure. In this way limiting values of settlement were determined and the ultimate pressures were taken from the other load-settlement curves. The footings at the surface failed at 10.5 per cent of the width, B. Settlement at ultimate load changed very little with depth from 10 inches to 40 inches;

settlements of 25.2 per cent B were found for 10 inches deep tests and 26 per cent B for 40 inches deep tests. Table 5 shows point load-settlement data for all 20 tests. Fig. 9 shows load-settlement curves for tests 20 inches and 40 inches deep.

Tests 1, 2, 3 and 16 were load tests of a 2 inch by 12 inch footing at the surface, with densities ranging from 84.0 to 96.4 lb/ft<sup>3</sup>. These tests served as a starting point for the other tests. Many similar tests have been made by other observers (9) (10), and the theoretical bearing capacity factor  $N_\gamma$  found to be in good agreement with experiment. In tests 16 ( $R_D = 0.8$ ), 1 ( $R_D = 0.69$ ), and 2 ( $R_D = 0.61$ ), the phenomenon called general shear failure occurred. When the soil under a footing fails in general shear, the load decreases rapidly, and the soil on one side (sometimes both) rises. Fig. 10a shows this in a photograph of test 16 after failure. The shear zone has come to the surface and is clearly visible and well-defined. Similar shear zones, smaller in extent, were observed for the less dense tests 1 and 2.

From these surface tests values of the dimensionless quantity,  $\frac{2q_{ult}}{\gamma B}$ , can be computed. A comparison of this quantity determined from the surface load tests is made with the theoretical factors  $N_\gamma$  in Fig. 11. To eliminate the effect of surcharge and cohesion it is necessary to make two corrections to the pressure at failure. The first is  $-qN_q$ , where  $q = (\text{density})(\text{settlement at failure})$ . This is small, of the order of 0.5 lb/in<sup>2</sup>. Of greater magnitude and importance is the correction  $-cN_c$ . The bearing capacity factor  $N_c$  varies from 33 to 72 for these tests. Unfortunately, the small cohesion of this air-dried sand cannot be measured easily, and is not known. Fig. 12b shows the portion of total

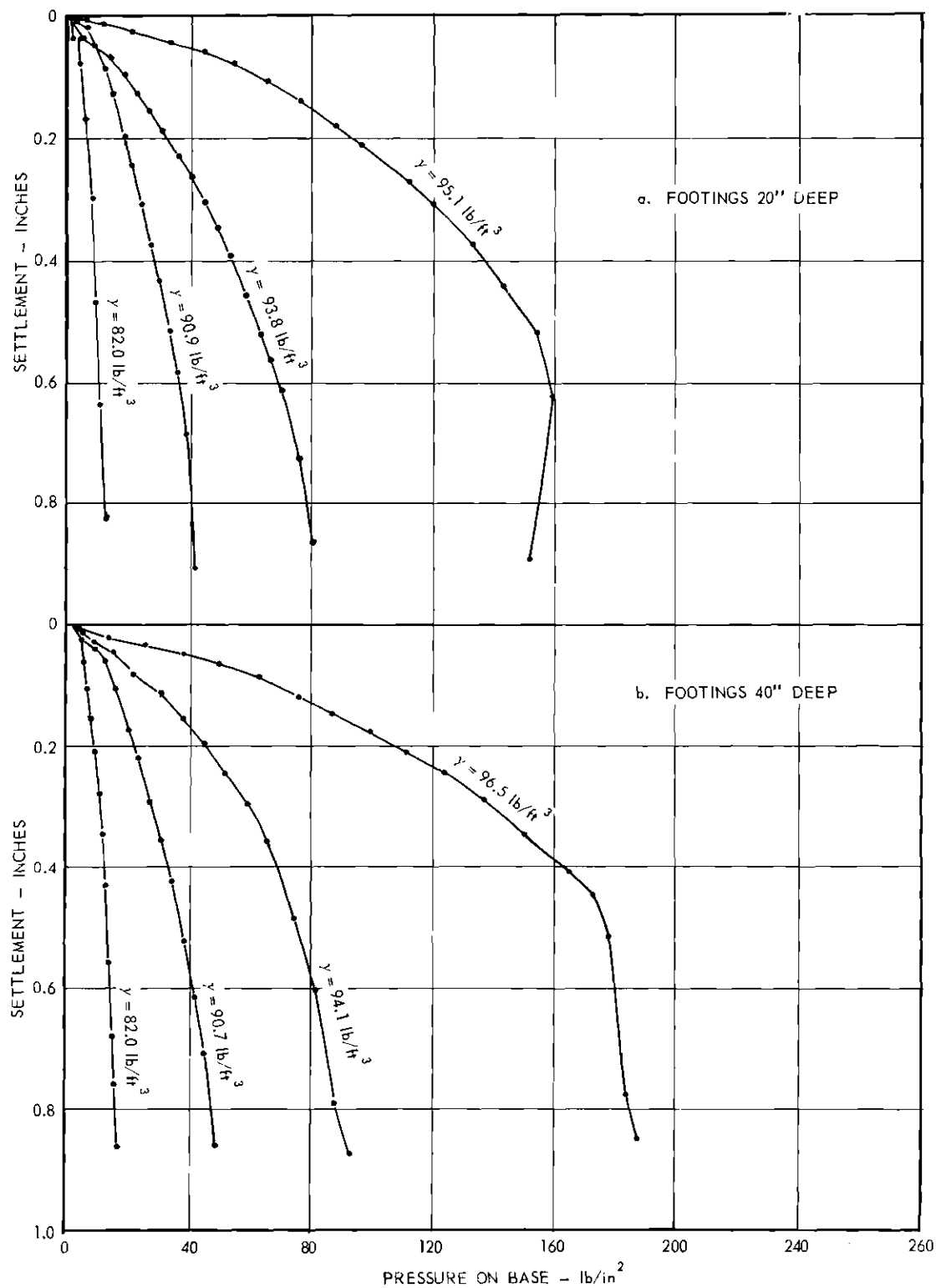
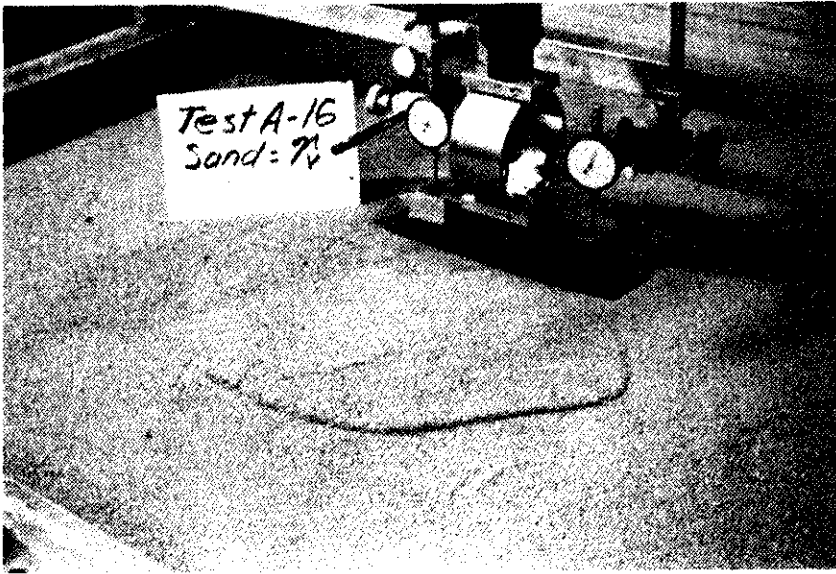
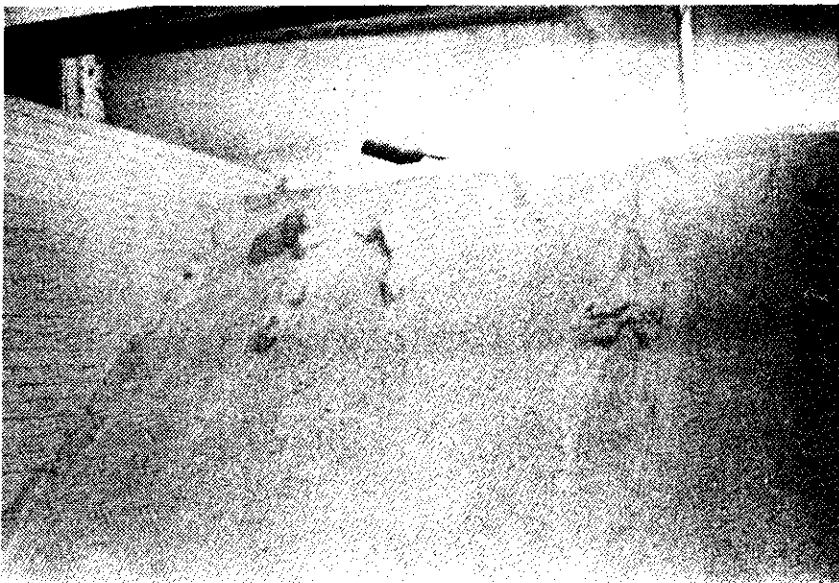


Figure 9. Load-Settlement Curves.



a. GENERAL SHEAR FAILURE



b. AN UNBRACED CUT IN THE SAND

Figure 10. Photographs a. General Shear Failure and b. an Unbraced Cut in the Sand.

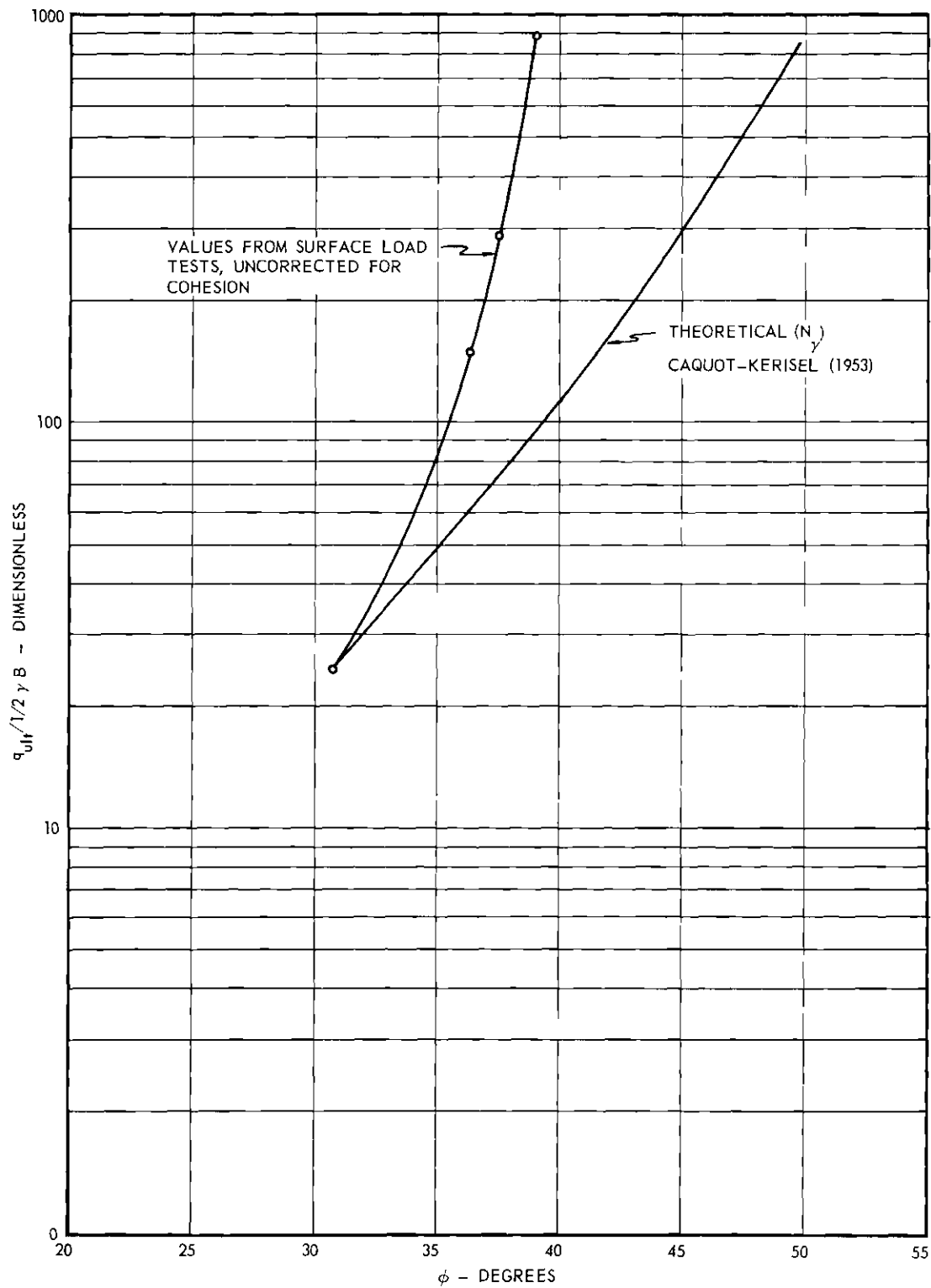


Figure 11. Comparison of Theoretical  $N_\gamma$  and Experimental Bearing Capacity Factor -  $q_{ult} / \frac{1}{2} \gamma B$ .

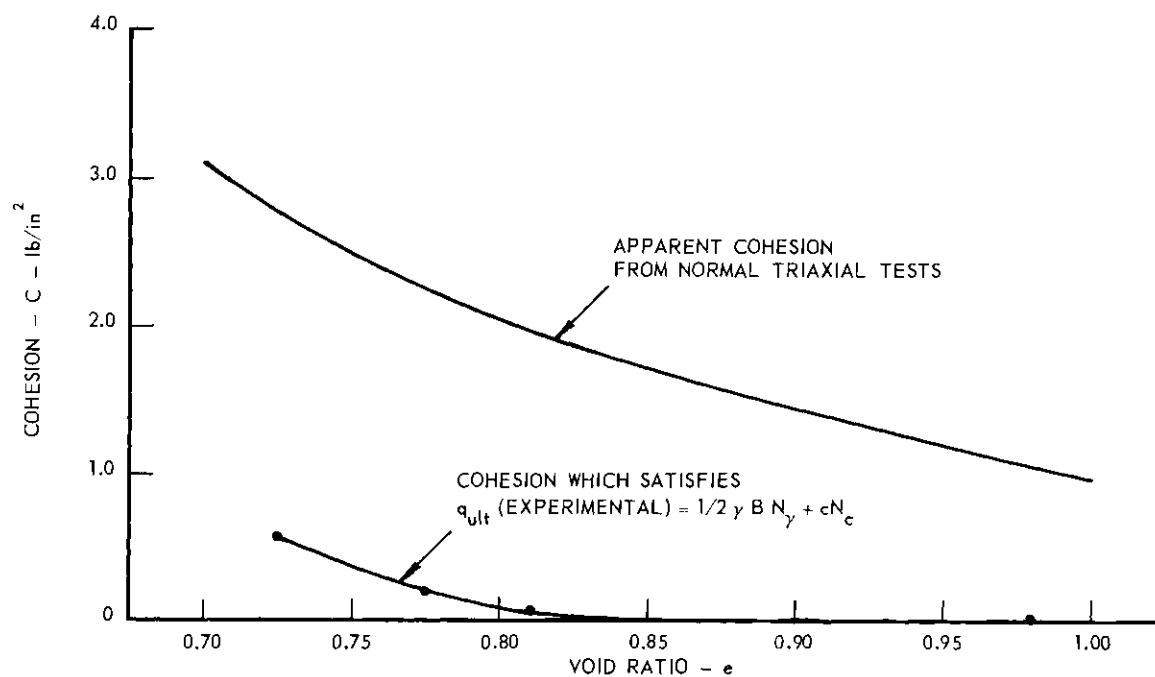


Figure 12a. Cohesion as a Function of Void Ratio.

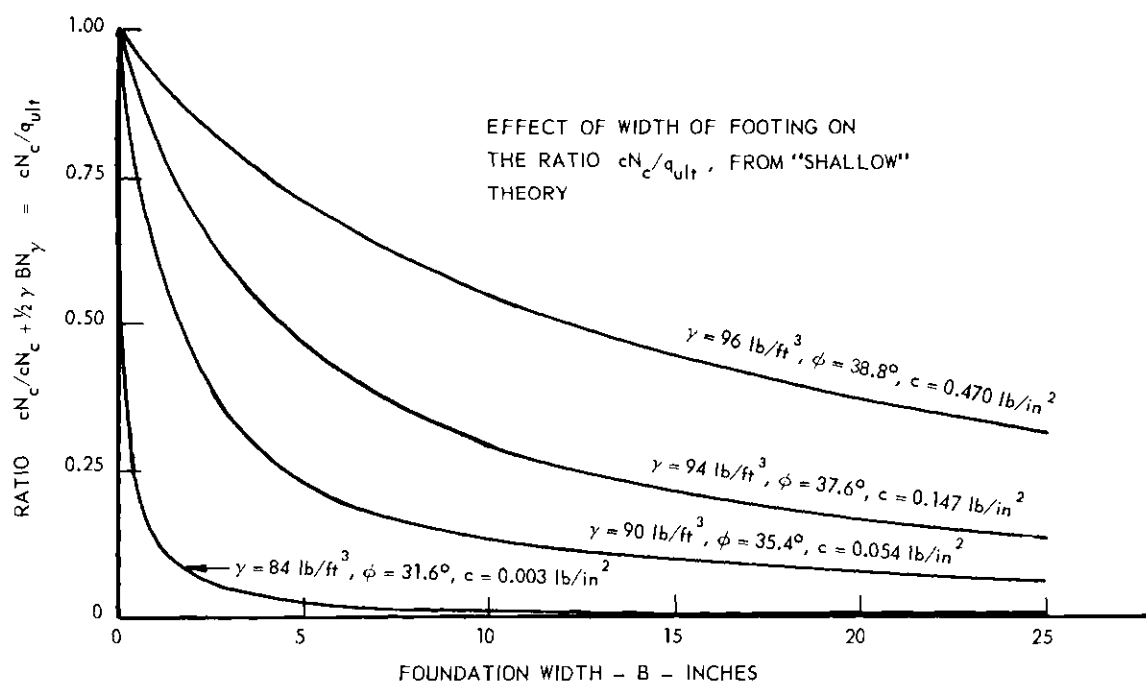


Figure 12b. Contribution of Cohesion to Bearing Capacity.

bearing capacity contributed by cohesion as a function of footing width. A cohesion as small as  $0.5 \text{ lb/in}^2$  can account for 85 per cent of total bearing capacity for a two-inch wide footing. In Fig. 12a are shown the values of cohesion which would make these surface load tests agree exactly with theoretical  $N_\gamma$  values. This cohesion is  $0.55 \text{ lb/in}^2$  for the least void ratio (0.725) and decreases rapidly to practically zero at  $e = 0.85$ . On the same figure is shown the apparent cohesion found from the triaxial tests. This cohesion is caused by the interlocking of grains, capillary forces, the membrane used and other factors in the triaxial tests which have not been accounted for (11). However, Chen has shown that even when all these factors are taken into account, there is still some small amount of cohesion which is a property of the sand. Terzaghi suggests the failure envelope is curved near the origin for dense sands. Representing a curved failure envelope by a single angle of internal friction,  $\phi$ , requires either a shear intercept greater than zero (cohesion) or an overestimation of strength at high normal stress, or both. Fig. 10b shows the sand in the box in which the models were built after the door was opened to empty it. The lines on the side of the box are one inch apart. It can be seen here that the sand will stand free vertically for about three inches. Although this is not an accurate measure of the amount of cohesion the sand possesses because of vibrations while the slope was forming, it shows that the sand does have some cohesion.

The 16 load tests numbered 4 through 20 with the exception of number 16, were load tests of footings beneath the surface. Table 1 gives a summary of the significant results of these tests.

Table 1. Summary of Significant Results from Footing Load Tests

| Test<br>No. | Footing<br>Width | Footing<br>Length | Depth    | Density               | Pressure<br>at<br>Failure | $\rho/B$<br>Corre-<br>sponding | $\frac{E_t}{1-\nu^2}$ | $\frac{E_{50}}{1-\nu^2}$ |
|-------------|------------------|-------------------|----------|-----------------------|---------------------------|--------------------------------|-----------------------|--------------------------|
|             | (inches)         | (inches)          | (inches) | (lb/ft <sup>3</sup> ) | (lb/in <sup>2</sup> )     | (per cent)                     | (lb/in <sup>2</sup> ) | (lb/in <sup>2</sup> )    |
| 16          | 2                | 12                | 0        | 96.4                  | 47.0                      | 10.5                           | 1370                  | 1110                     |
| 1           | 2                | 12                | 0        | 93.6                  | 14.5                      | 10.5                           | 309                   | 280                      |
| 2           | 2                | 12                | 0        | 91.9                  | 7.8                       | 10.5                           | 154                   | 153                      |
| 3           | 2                | 12                | 0        | 84.0                  | 1.4                       | 10.5                           | 29                    | 28                       |
| 17          | 2.44             | 12.44             | 10       | 95.0                  | 126                       | 25.2                           | 3600                  | 1270                     |
| 4           | 2                | 12                | 10       | 94.0                  | 48.5                      | 25.2                           | 660                   | 417                      |
| 5           | 2                | 12                | 10       | 91.1                  | 27.0                      | 25.2                           | 386                   | 231                      |
| 6           | 2                | 12                | 10       | 83.8                  | 8.0                       | 25.2                           | 80                    | 67                       |
| 18          | 2.44             | 12.44             | 20       | 95.1                  | 160                       | 25.6                           | 3300                  | 1540                     |
| 7           | 2.44             | 12.44             | 20       | 93.8                  | 71                        | 25.6                           | 1360                  | 605                      |
| 8           | 2.44             | 12.44             | 20       | 90.9                  | 37.5                      | 25.6                           | 960                   | 309                      |
| 9           | 2.44             | 12.44             | 20       | 82.0                  | 11.1                      | 25.6                           | 183                   | 101                      |
| 19          | 2.44             | 12.44             | 30       | 96.4                  | 178                       | 25.8                           | 3640                  | 1640                     |
| 10          | 2.44             | 12.44             | 30       | 94.2                  | 81.0                      | 25.8                           | 2060                  | 795                      |
| 11          | 2.44             | 12.44             | 30       | 91.8                  | 44.0                      | 25.8                           | 1710                  | 365                      |
| 12          | 2.44             | 12.44             | 30       | 82.0                  | 12.3                      | 25.8                           | 320                   | 114                      |
| 20          | 2.44             | 12.44             | 40       | 96.5                  | 185                       | 26.0                           | 4640                  | 1815                     |
| 13          | 2.44             | 12.44             | 40       | 94.1                  | 82.8                      | 26.0                           | 1470                  | 775                      |
| 14          | 2.44             | 12.44             | 40       | 90.7                  | 42.5                      | 26.0                           | 1750                  | 365                      |
| 15          | 2.44             | 12.44             | 40       | 82.0                  | 14.2                      | 26.0                           | 447                   | 139                      |



Of these tests only numbers 17 and 18, the most dense tests 10 and 20 inches deep, showed a true ultimate pressure. Load-settlement curves for tests 20 inches and 40 inches deep are shown in Fig. 9. In none of these tests did any shear appear at the surface. When the soil failed under the footing in test 17, however, the footing began to move laterally at the top perpendicular to its longer axis. A passive Rankine zone formed on one side of the footing and an active Rankine zone formed on the other. This was most probably because the rupture zone shown in Fig. 1d had formed to a limited extent and the wedge and the base of the foundation with it were traveling along one of the boundaries of this shear zone. This caused the base of this foundation to move laterally as well as vertically down, and the top of the foundation to move laterally in the opposite direction.

A comparison of the theoretical and experimental ultimate pressures with depth is made in Fig. 13. These were determined by first plotting ultimate pressure against density for each depth, drawing smooth curves through the points, and then picking off the values plotted in Fig. 13. This was necessary because there was some variation in density between different models even though they were formed by the same method. The theory used for this comparison is the "shallow" theory (12) which is usually applied to footings at the surface and depths of one foundation width or less. It does not take into account any of the strength of the soil above the level of the base of the footing and so gives  $N_q$  values which are considerably less than those from the "deep" theories. The "deep" theory which gives the largest  $N_q$  values was presented by Meyerhof (13), the one which gives the smallest values of  $N_q$  was presented

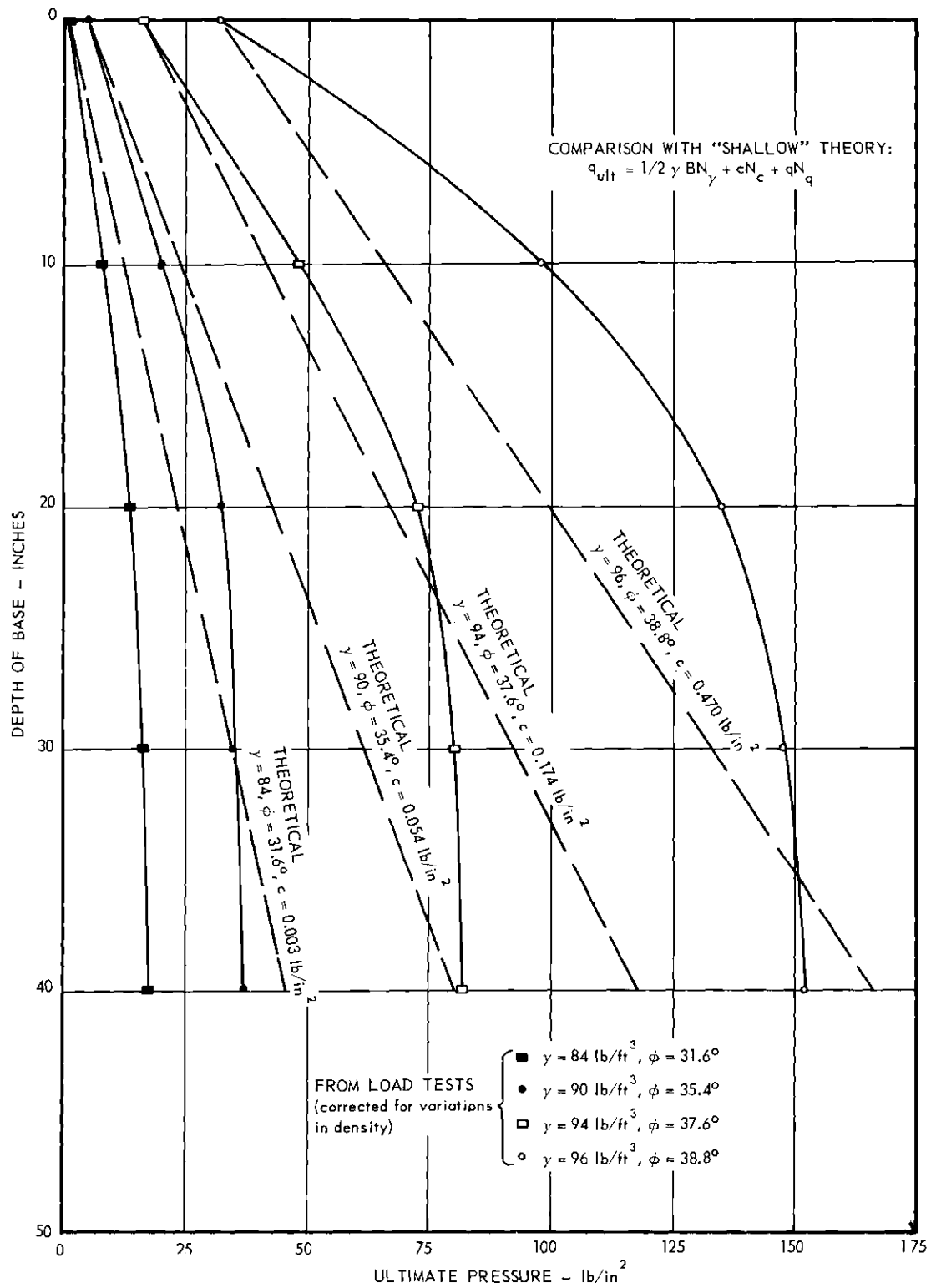


Figure 13. Ultimate Bearing Capacity as a Function of Depth.

by Hansen (14). Shallow  $N_q$ 's are from 12 per cent to 37 per cent for  $\phi = 30^\circ$  and from 2.9 per cent to 34 per cent for  $\phi = 45^\circ$  of the  $N_q$  values from deep theories, depending on which theory is chosen for comparison.

However, as can be seen in Fig. 13, even the shallow theory overestimates the bearing capacity after some depth. The reason for this dissonance is not in the quantitative values yielded by the theory, but in the fact that theory predicts a linear increase of bearing capacity with depth. Bearing capacity of this sand as determined by these tests increases with depth at a constantly decreasing rate. There is no theory which predicts an ultimate bearing capacity regardless of depth, nor one which predicts an increase at nearly such a slow rate as indicated by the final slopes of the curves shown in Fig. 13. These curves show that  $N_q$  decreases constantly with depth. Average  $N_q$  values for the first and last ten inches are shown in Table 2 below. These values were determined by dividing the increase in bearing capacity by the increase in vertical pressure.

Table 2. Average  $N_q$  Values

|                                   |      |      |      |      |
|-----------------------------------|------|------|------|------|
| $\gamma$<br>(lb/ft <sup>3</sup> ) | 84   | 90   | 94   | 96   |
| $\phi$<br>(degrees)               | 31.6 | 35.4 | 37.6 | 38.8 |
| Avg. $N_q$ for<br>0-10 inches     | 14   | 29   | 59   | 115  |
| Avg. $N_q$ for<br>30-40 inches    | 3.3  | 3.8  | 4.6  | 8.1  |

The two curves for the greatest densities, 94 and 96 lb/ft<sup>3</sup>, show agreement with the corresponding theoretical straight lines at one point beneath the surface. These theoretical curves were drawn assuming that the sand actually possesses the amount of cohesion necessary to satisfy

$$q_{ult}(\text{experimental}) = cN_c + \frac{1}{2}\gamma B N_\gamma$$

where  $q_{ult}$  is from the surface tests. If the cohesion had been measured and was not equal to the cohesion assumed, the theoretical curves would be shifted either right or left, changing the depth at which theory and experiment are in agreement. The curves for densities of 84 and 90 lb/ft<sup>3</sup> lie below the corresponding theoretical curves at all depths beneath the surface. The relative densities for these densities are 0.25 and 0.54 respectively. Various empirical corrections have been suggested, to be made to the angle  $\phi$  or to bearing capacity directly, which would make theoretical (corrected) bearing capacity agree with observed values. Using  $N_q$  for the upper ten inches as shown in Table 1 angles  $\phi$  can be found which correspond. We can call this angle  $\phi_E$  for effective angle of internal friction. These values, with the relative density and the ratio of  $\phi_E$  to the angle of internal friction,  $\phi$  from normal triaxial tests are shown in Table 3.

The slopes of the depth-pressure curves or rate of increase of bearing capacity indicated by these  $N_q$  values are those which would apply to foundations in this sand at a depth  $5B$  or less.

Table 3. Angle of Friction  $\phi_E$  Deduced from Load Tests.  
(Upper ten inches only)

| $R_D$<br>Relative<br>Density<br>(dimensionless) | $N_q$<br>Experimental<br>(dimensionless) | $\phi_E$<br>(degrees) | $\phi_E/\phi$<br>(dimensionless) |
|---|--|-----------------------|----------------------------------|
| 0.78  | 115                                      | 44                    | 1.13                             |
| 0.71  | 59                                       | 39.4                  | 1.05                             |
| 0.54  | 29                                       | 33.8                  | 0.95                             |
| 0.25  | 14                                       | 28.5                  | 0.90                             |

Fig. 14 shows the ratio  $\phi_E/\phi$  as a function of relative density. Also shown in this figure is the curve

$$\phi_E/\phi = 0.90 + 0.61(R_D)^4$$

which is a good approximation of the observed values over the range of measurement. The number of observations is too small to warrant suggestion of this expression for general use.

In Fig. 13 it can be seen that after a depth of about 20 inches (approximately 8B) there is little increase of bearing capacity with depth. From this depth to 40 inches there is at most a 27 per cent increase in bearing (for  $\gamma = 84 \text{ lb/ft}^3$ ) and the increase is only 12 per cent for  $\gamma = 96 \text{ lb/ft}^3$ .

The penetrometer soundings which were made primarily as a check on the density are themselves load tests of very small footings. The procedure is different, however, in that load settlement data are not

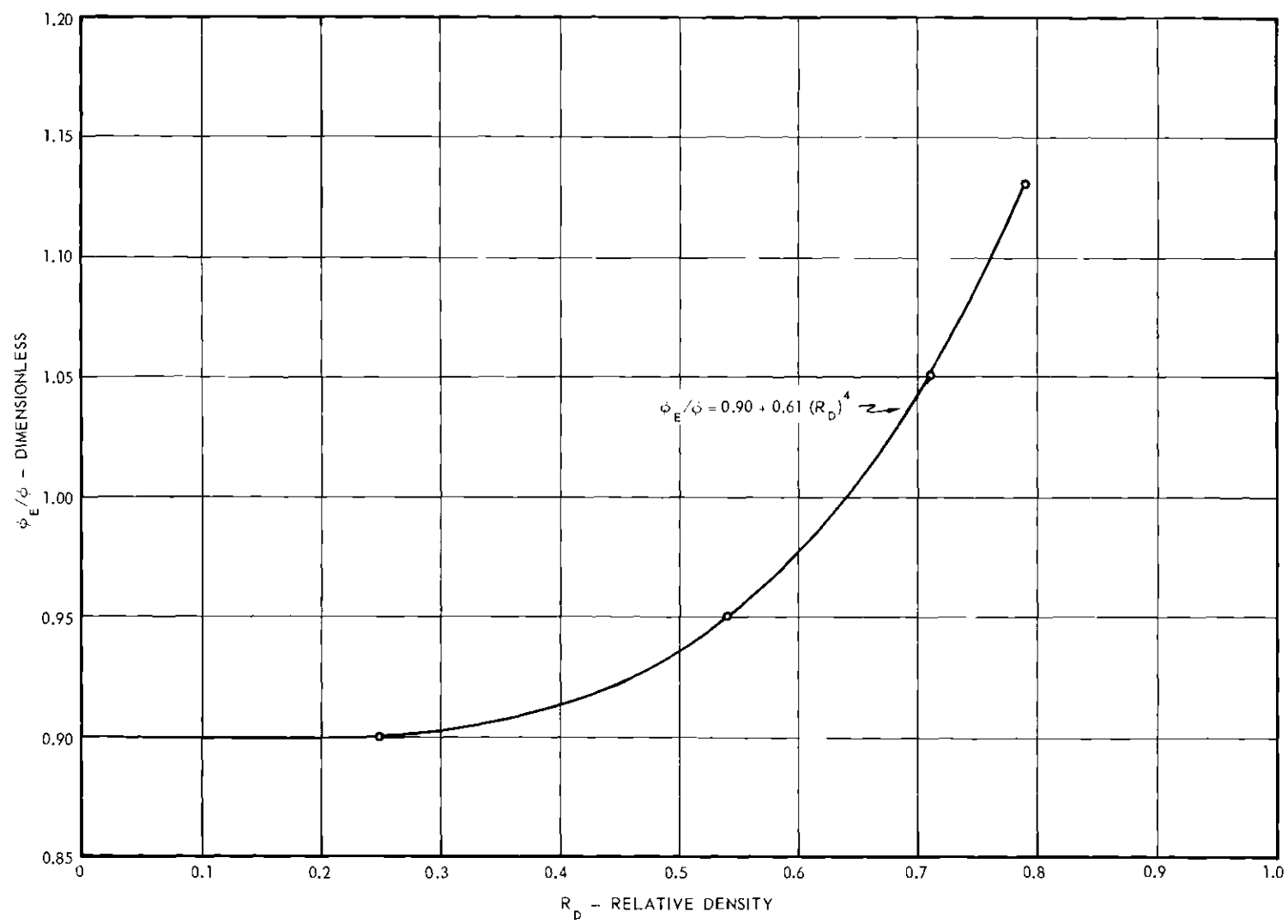


Figure 14. Ratio  $\phi_E / \phi$  as a Function of Relative Density.

recorded as they are in a footing load test, where settlement is measured very carefully and the load applied in increments. The soundings are performed by pushing the penetrometer at a constant rate and recording the average force required to push it for each inch which it penetrates. This load is then converted to pressure on the point and is plotted against depth.

A comparison is made in Fig. 15 between bearing capacity and penetration resistance. It can be seen that at a depth of 40 inches the ultimate bearing capacity is only from 25 per cent to 50 per cent of resistance to penetration, the difference between the two increasing with density.

There is an essential difference between these two types of tests, and the results are not directly comparable. In the footing load tests, the ultimate pressure or bearing capacity was chosen as that load which corresponded to some limiting value of settlement. In determination of resistance to penetration, settlement is not involved. Thus it is certain that for the same size loaded area, whether penetrometer or footing, that resistance to penetration will be greater than bearing capacity.

Recently evidence has been found that resistance to penetration is a function of the size of the penetrometer, higher unit resistance being realized for smaller penetrometers (15).

Table 4 gives the ultimate unit skin friction  $q_s$  and settlement at failure for all tests in which skin friction was measured. As explained in Chapter I, skin friction is usually rationally computed by

$$q_s = \frac{1}{2} \gamma D K_s \alpha \tan \phi$$

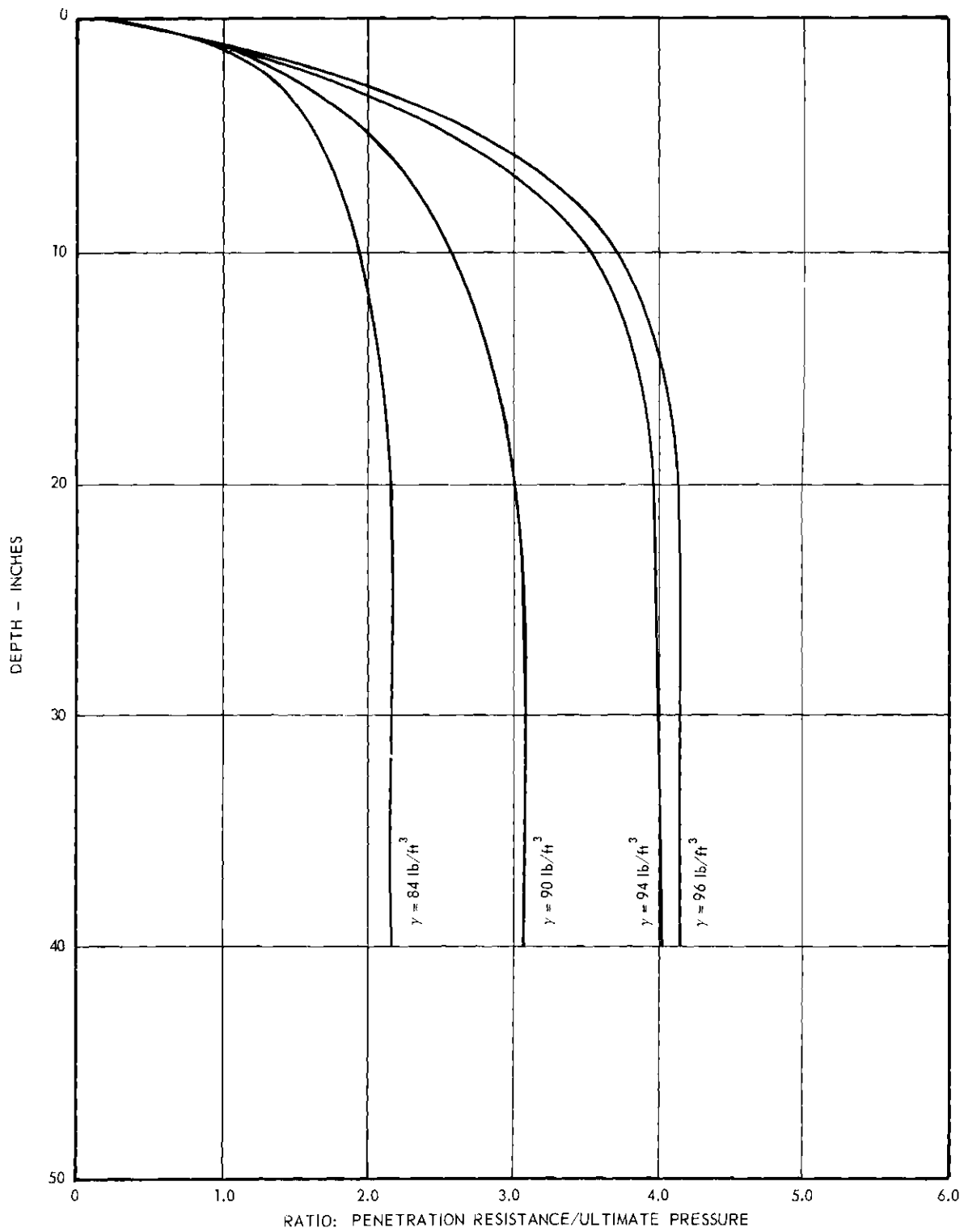


Figure 15. Comparison of Ultimate Bearing Capacity and Penetration Resistance.



Table 4. Summary of Results from Skin Load Tests

| Test No. | Depth<br>(inches) | Density<br>(lb/ft <sup>3</sup> ) | Skin Friction<br>(lb/in <sup>2</sup> ) | Settlement<br>Corresponding<br>(inches) | Coefficient***<br>of Skin<br>Pressure, $k_s$ |
|----------|-------------------|----------------------------------|--|---|--|
| 18       | 20                | 95.1                             | 0.272                                  | 0.07                                    | 0.640  |
| 7        | 20                | 93.8                             | 0.169                                  | 0.13                                    | 0.424  |
| 8        | 20                | 90.9                             | 0.148                                  | 0.14                                    | 0.428  |
| 9        | 20                | 82.0                             | 0.125                                  | 0.10                                    | 0.449  |
| 19       | 30                | 96.4                             | 0.455                                  | 0.10                                    | 0.70   |
|          |                   |                                  | 0.160*                                 | 0.04                                    | 0.246  |
| 10       | 30                | 94.2                             | 0.283                                  | 0.19                                    | 0.465  |
| 11       | 30                | 91.8                             | 0.210                                  | 0.17                                    | 0.398  |
| 12       | 30                | 82.0                             | 0.152                                  | 0.16                                    | 0.357  |
| 20       | 40                | 96.5                             | 0.675                                  | 0.15                                    | 0.775  |
|          |                   |                                  | 0.205*                                 | 0.04                                    | 0.235  |
|          |                   |                                  | 0.265**                                | 0.17                                    | 0.304  |
| 13       | 40                | 94.1                             | 0.270                                  | 0.11                                    | 0.330  |
| 14       | 40                | 90.7                             | 0.210                                  | 0.12                                    | 0.296  |
| 15       | 40                | 82.0                             | 0.188                                  | 0.15                                    | 0.328  |

\* Pulled after pushing

\*\* Pushed again after pulling

\*\*\* Computed assuming  $\alpha = 1.0$ .

If it is assumed that  $\alpha = 1$ , values of  $k_s$  may be computed from the above expression. Table 4 also includes  $k_s$  computed in this way. It may be noted that  $k_s$  generally decreases with density, from an average of 0.71 for  $\gamma = 96 \text{ lb/ft}^3$  to 0.38 for  $\gamma = 84 \text{ lb/ft}^3$ . The average  $k_s$  values for  $\gamma = 90 \text{ lb/ft}^3$  and  $\gamma = 94 \text{ lb/ft}^3$  are 0.38 and 0.41 respectively. Thus  $k_s$  seems to depend on the method of placing the sand for the most part. The high values of  $k_s$  for the compacted sand are in agreement with values of  $k_o$  noted by Terzaghi (16) and Tschebotarioff (17).  $k_o$  and  $k_s$  are different coefficients of earth pressure.  $k_o$  is the coefficient of earth pressure at rest, the ratio  $\sigma_3/\sigma_1$  where  $\sigma_3$  acts in a horizontal direction inside an earth mass.  $k_s$  is the coefficient of pressure which acts at an angle to the horizontal on the lateral surface of a foundation. It seems, however, that they are of the same order and probably subject to the same influences, i.e., wedging in of sand grains during compaction.

The results of three tests to measure skin friction, not conducted in the ordinary manner, are also reported in Table 4. Those values marked \* were determined by pulling the skin up after all other load tests were completed, and the one marked \*\* was determined by measuring the force required to push the skin a second time after pulling it. These tests showed  $q_s$  values which were considerably less than those determined on the initial loading. This indicates that the structure of the sand placed with vibration is disturbed by pulling the foundation up, and skin friction measured this way is lower than that which acts during initial loading. Complete skin load settlement data are given in Table 6.

A comparison was made of the force required to push the point and skin separately and that required to push point and skin together. The latter would be expected to be greater, because the pressure generally continues to increase with depth as explained above. The force required to push point and skin together was from 101 per cent to 129 per cent of the sum of the forces required to push them separately. The average was 122 per cent. This fact seems to exclude the possibility that there was a large amount of mechanical friction between the two sections of the model footing. This was also indicated by the smooth settlement of the skin under load, evidenced by the general smoothness of skin load-settlement curves.

Also computed from the point load settlement curves was the quantity  $E/(1 - \nu^2)$ . This quantity is used for the prediction of immediate settlement of foundations by

$$\rho = q B \frac{1 - \nu^2}{E} I_\rho$$

Where the load settlement curve is known,  $E/(1 - \nu^2)$  may be deduced. Two values of  $E/(1 - \nu^2)$  were computed; an initial tangent modulus  $E_t/(1 - \nu^2)$  and a secant modulus  $E_{50}/(1 - \nu^2)$  for the first 50 per cent of the load settlement curve. Values of  $I_\rho$  of 1.7 for the 2 inch by 12 inch footings and 1.6 for the 2.44 inch by 12.44 inch footings were used in computations. Since  $\nu$  has limiting values of 0 and 0.5 for real materials,  $E$  can be computed within a maximum error of  $\pm 15$  per cent by assuming  $1 - \nu^2 = 0.88$  (corresponding to  $\nu = 0.38$ ). Comparison of the values of  $E$  found in this way with those shown in Fig. 7 show that the ratio

$\sigma_1/\sigma_3$  must have been about 4 or greater for surface tests and about 3.5 for the deepest tests, intermediate values applying to intermediate depths.  $E/1 - \nu^2$  as a function of depth is shown in Fig. 16.

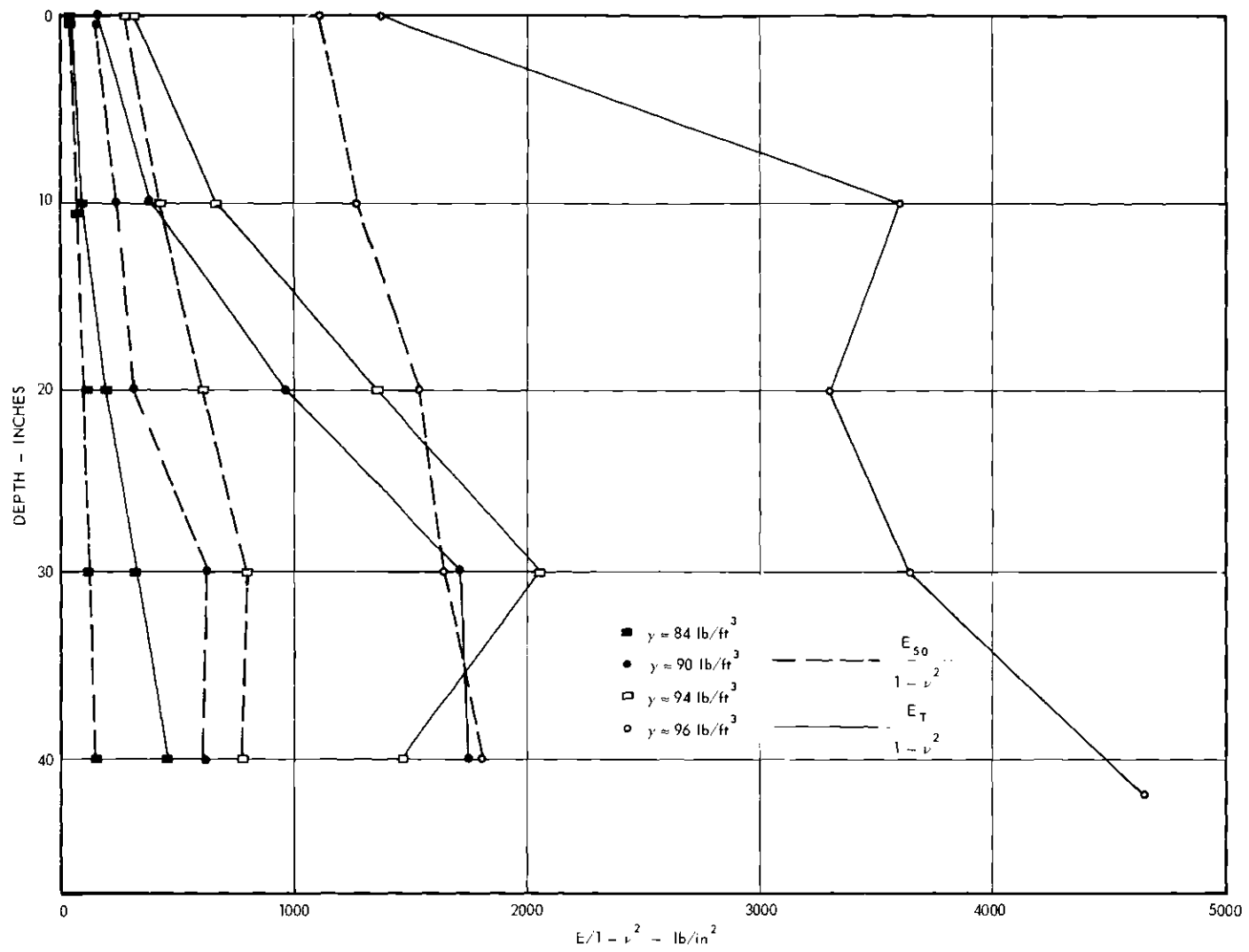


Figure 16.  $E/(1 - \nu^2)$  as a Function of Depth.

## CHAPTER IV

## CONCLUSIONS

(1) For a foundation buried in a relatively homogeneous mass of sand, bearing capacity increases with depth at a constantly decreasing rate.

(2) Unit resistance to penetration determined by a small diameter penetrometer may be as much as four or five times as great as the ultimate bearing capacity of a model footing, the difference increasing both with relative density and depth.

(3) Estimates of skin friction made by pulling a foundation up may give apparent values of  $q_s$  which are as little as 30 per cent of the skin friction which acts when the foundation is pushed.

## CHAPTER V

## RECOMMENDATIONS

(1) Load tests for determination of ultimate bearing capacity should be made on other sands. This will aid in the separation of the effects of changes in angle of internal friction and changes in relative density.

(2) Larger model tests in this same sand should be made, as well as penetrometer soundings with a larger penetrometer. These investigations should attempt to find the effects of actual size of the footing or penetrometer, and the importance of the depth ratio,  $D/B$ .

(3) Tests of a qualitative nature should be performed to discover the phenomenon which occurs when a deep foundation fails.

## APPENDIX



## NOTATION

|                  |   |
|------------------|---|
| B                | = width of footing (inches)   |
| c                | = cohesion in Coulomb's equation ( $\text{lb/in}^2$ )   |
| D                | = depth of base of foundation (inches)  |
| $E_t$            | = initial tangent modulus of deformation ( $\text{lb/in}^2$ )   |
| $E_{50}$         | = secant modulus of deformation for the first 50 per cent of a load-settlement curve ( $\text{lb/in}^2$ ) |
| e                | = void ratio  |
| $e_{\max}$       | = void ratio in loosest state   |
| $e_{\min}$       | = void ratio in densest state   |
| $I_p$            | = influence value for settlement  |
| K                | = ratio of major to minor principal stress  |
| $K_s$            | = coefficient of skin pressure  |
| m                | = ratio of adhesion to cohesion   |
| $N_c$            | = bearing capacity factor   |
| $N_q$            | = bearing capacity factor   |
| N                | = bearing capacity factor   |
| $Q_p$            | = point load on a deep foundation (lbs)   |
| $Q_s$            | = skin load on a deep foundation (lbs)  |
| $Q_t$            | = total load on a deep foundation (lbs)   |
| $q_p$            | = unit point resistance of a deep foundation ( $\text{lb/in}^2$ )   |
| $q_s$            | = unit skin resistance of a deep foundation ( $\text{lb/in}^2$ )  |
| $q_{\text{ult}}$ | = ultimate pressure the soil can exert on the base of the foundation ( $\text{lb/in}^2$ )                 |

## NOTATIONS (Continued)

$R_D$  = relative density (  $(e_{\max} - e) / (e_{\max} - e_{\min})$  )

$V$  = total vertical load on a shallow footing (lbs)

$\alpha$  = ratio of  $\tan \delta$  to  $\tan \phi$

$\gamma$  = unit weight (lb/ft<sup>3</sup>)

$\delta$  = angle of friction between the sand and the lateral surface of  
a deep foundation (degrees)

$\nu$  = Poisson's ratio

$\rho$  = settlement (inches)

$\bar{\sigma}$  = effective normal stress (lb/in<sup>2</sup>) (bar may be omitted)

$\sigma_1, \sigma_3$  = major, minor principal stress (lb/in<sup>2</sup>)

$\phi$  = angle of internal friction (degrees)

$\psi$  = angle (degrees)

$\sim$  means approximately

Table 5. Load-Settlement Data for Point Loads

Test No. 1  
 2 inches x 12 inches  
 At surface  
 Density 93.6 lb/ft<sup>3</sup>

| Pressure<br>on Base<br>(lb/in <sup>2</sup> ) | Deflection<br>( $\frac{\text{inches}}{10,000}$ ) |
|--|--|
| 0.00   | 0  |
| 0.93   | 159  |
| 1.85   | 261  |
| 2.78   | 360  |
| 3.70   | 461  |
| 4.63   | 537  |
| 5.55   | 666  |
| 6.46   | 740  |
| 7.40   | 902  |
| 8.26   | 1027   |
| 9.29   | 1213   |
| 10.20  | 1370   |
| 11.10  | 1517   |
| 12.05  | 1690   |
| 12.95  | 1845   |
| 13.90  | 2030   |
| 14.80  | 2195   |
| 15.75  | 2397   |
| 16.62  | 2572   |
| 17.60  | 2770   |
| 18.48  | 3007   |
| 19.40  | 3170   |
| 20.30  | 3570   |
| 21.20  | 3855   |
| 22.20  | 4025   |
| 8.15   |  |

Test No. 2  
 2 inches x 12 inches  
 At surface  
 Density 91.9 lb/ft<sup>3</sup>

| Pressure<br>on Base<br>(lb/in <sup>2</sup> ) | Deflection<br>( $\frac{\text{inches}}{10,000}$ ) |
|--|--|
| 0.00   | 0  |
| 0.46   | 138  |
| 0.94   | 244  |
| 1.39   | 340  |
| 1.85   | 445  |
| 2.34   | 545  |
| 2.80   | 640  |
| 3.24   | 734  |
| 3.70   | 864  |
| 4.20   | 962  |
| 4.63   | 1055   |
| 5.10   | 1175   |
| 5.50   | 1300   |
| 6.05   | 1457   |
| 6.54   | 1585   |
| 6.94   | 1706   |
| 7.41   | 1862   |
| 7.85   | 2027   |
| 8.35   | 2202   |
| 8.77   | 2378   |
| 9.27   | 2600   |
| 9.66   | 2753   |
| 10.20  | 3043   |
| 10.57  | 3271   |
| 11.10  | 3611   |
| 11.60  | 4070   |
| 11.10  | 5870   |
| 8.90   | 8385   |

Table 5 (Continued)

Test No.3  
 2 inches x 12 inches  
 At surface  
 Density 84.0 lb/ft<sup>3</sup>

| Pressure<br>on Base<br>(lb/in <sup>2</sup> ) | Deflection<br>( <u>inches</u><br>10,000) |
|--|--|
| 0.00   | 0  |
| 0.12   | 80                                       |
| 0.24   | 225                                      |
| 0.35   | 385                                      |
| 0.48   | 540                                      |
| 0.60   | 737                                      |
| 0.71   | 928                                      |
| 0.83   | 1125                                     |
| 0.95   | 1315                                     |
| 1.08   | 1495                                     |
| 1.20   | 1707                                     |
| 1.32   | 1885                                     |
| 1.42   | 2175                                     |
| 1.56   | 2355                                     |
| 1.66   | 2576                                     |
| 1.77   | 2890                                     |
| 1.92   | 3252                                     |
| 2.04   | 3531                                     |
| 2.14   | 3862                                     |
| 2.29   | 4230                                     |
| 2.37   | 4570                                     |
| 2.49   | 4964                                     |
| 2.62   | 5400                                     |
| 2.73   | 5790                                     |
| 2.87   | 6252                                     |
| 2.99   | 6700                                     |
| 3.12   | 7135                                     |
| 3.22   | 7515                                     |
| 3.34   | 7890                                     |
| 3.48   | 8300                                     |
| 3.55   | 8650                                     |
| 3.70   | 9132                                     |
| 3.82   | 9570                                     |
| 3.92   | 9935                                     |
| 4.05   | 10570                                    |
| 4.16   | 10725                                    |
| 4.30   | 11600                                    |
| 4.42   | 12190                                    |
| 4.52   | 12300                                    |

Test No. 4  
 2 inches x 12 inches  
 At surface  
 Density 94.0 lb/ft<sup>3</sup>

| Pressure<br>on Base<br>(lb/in <sup>2</sup> ) | Deflection<br>( <u>inches</u><br>10,000) |
|--|--|
| 1.0  | 0  |
| 4.7  | 586                                      |
| 8.2  | 807                                      |
| 11.9   | 1042                                     |
| 15.6   | 1340                                     |
| 19.2   | 1606                                     |
| 23.1   | 1950                                     |
| 27.2   | 2400                                     |
| 30.6   | 2737                                     |
| 34.4   | 3240                                     |
| 37.2   | 3601                                     |
| 42.2   | 4270                                     |
| 45.5   | 4750                                     |
| 49.4   | 5496                                     |
| 52.8   | 6195                                     |
| 53.6   | 8418                                     |
| 55.1   | 12432                                    |

Table 5 (Continued)

Test No. 5  
 2 inches x 12 inches  
 10 inches Deep  
 Density 91.1 lb/ft<sup>3</sup>

| Pressure<br>on Base<br>(lb/in <sup>2</sup> ) | Deflection<br>( <u>inches</u><br>10,000) |
|--|--|
| 1.22   | 0  |
| 3.04   | 94                                       |
| 4.70   | 241                                      |
| 6.13   | 412                                      |
| 8.24   | 649                                      |
| 10.25  | 985                                      |
| 11.90  | 1284                                     |
| 13.90  | 1604                                     |
| 15.60  | 1931                                     |
| 18.40  | 2408                                     |
| 19.70  | 2658                                     |
| 21.90  | 3168                                     |
| 23.30  | 3469                                     |
| 25.10  | 4036                                     |
| 26.20  | 4450                                     |
| 29.20  | 5470                                     |
| 30.90  | 6080                                     |
| 32.40  | 6919                                     |
| 33.80  | 8573                                     |
| 36.00  | 10920                                    |
| 38.30  | 12785                                    |

Test No. 6  
 2 inches x 12 inches  
 10 inches Deep  
 Density 83.8 lb/ft<sup>3</sup>

| Pressure<br>on Base<br>(lb/in <sup>2</sup> ) | Deflection<br>( <u>inches</u><br>10,000) |
|--|--|
| 1.0  | 0  |
| 1.57   | 253                                      |
| 2.11   | 480                                      |
| 2.69   | 710                                      |
| 3.22   | 1025                                     |
| 3.85   | 1465                                     |
| 4.34   | 1772                                     |
| 4.91   | 2253                                     |
| 5.47   | 2669                                     |
| 5.89   | 3175                                     |
| 6.57   | 3572                                     |
| 7.07   | 3957                                     |
| 7.70   | 4505                                     |
| 8.19   | 4940                                     |
| 8.81   | 5540                                     |
| 9.42   | 6340                                     |
| 9.92   | 6760                                     |
| 10.40  | 7280                                     |
| 10.95  | 8048                                     |
| 11.56  | 8502                                     |
| 12.10  | 9222                                     |
| 12.60  | 10122                                    |
| 13.15  | 10787                                    |
| 13.75  | 11897                                    |
| 14.21  | 13102                                    |

Table 5 (Continued)

Test No. 7  
 2.44 inches x 12.44 inches  
 20 inches Deep  
 Density 93.8 lb/ft<sup>3</sup>

| Pressure<br>on Base<br>(lb/in <sup>2</sup> ) | Deflection<br>( <u>inches</u><br>10,000) |
|--|--|
| 1.00   | 0  |
| 5.50   | 365                                      |
| 9.90   | 491                                      |
| 14.20  | 698                                      |
| 18.90  | 973                                      |
| 23.00  | 1291                                     |
| 27.30  | 1553                                     |
| 31.70  | 1879                                     |
| 36.40  | 2283                                     |
| 40.60  | 2620                                     |
| 45.80  | 3060                                     |
| 49.50  | 3466                                     |
| 53.50  | 3911                                     |
| 59.10  | 4583                                     |
| 63.70  | 5215                                     |
| 67.30  | 5658                                     |
| 70.20  | 6194                                     |
| 76.50  | 7265                                     |
| 80.50  | 8631                                     |
| 84.20  | 12921                                    |

Test No. 8  
 2.44 inches x 12.44 inches  
 20 inches Deep  
 Density 90.9 lb/ft<sup>3</sup>

| Pressure<br>on Base<br>(lb/in <sup>2</sup> ) | Deflection<br>( <u>inches</u><br>10,000) |
|--|--|
| 1.0  | 0  |
| 3.9  | 85                                       |
| 6.6  | 193                                      |
| 9.6  | 461                                      |
| 12.5   | 855                                      |
| 15.5   | 1309                                     |
| 19.3   | 1980                                     |
| 21.6   | 2415                                     |
| 24.5   | 3072                                     |
| 27.6   | 3744                                     |
| 30.6   | 4361                                     |
| 33.5   | 5152                                     |
| 35.8   | 5822                                     |
| 39.4   | 6866                                     |
| 42.0   | 9082                                     |
| 44.9   | 10874                                    |
| 47.0   | 13030                                    |
| 50.0   | 14402                                    |

Table 5 (Continued)

Test No. 9  
 2.44 inches x 12.44 inches  
 20 inches Deep  
 Density 82.0 lb/ft<sup>3</sup>

| Pressure<br>on Base<br>(lb/in <sup>2</sup> ) | Deflection<br>(inches<br>10,000) |
|--|----------------------------------|
| 1.00   | 0                                |
| 2.50   | 341                              |
| 3.90   | 373                              |
| 5.30   | 760                              |
| 6.75   | 1677                             |
| 8.20   | 2976                             |
| 9.80   | 4681                             |
| 11.10  | 6370                             |
| 12.60  | 8245                             |
| 13.50  | 9375                             |
| 14.20  | 10792                            |
| 15.10  | 11850                            |
| 15.90  | 12737                            |

Test No. 10  
 2.44 inches x 12.44 inches  
 30 inches Deep  
 Density 94.2 lb/ft<sup>3</sup>

| Pressure<br>on Base<br>(lb/in <sup>2</sup> ) | Deflection<br>(inches<br>10,000) |
|--|----------------------------------|
| 1.2  | 0                                |
| 6.2  | 40                               |
| 11.4   | 92                               |
| 15.6   | 218                              |
| 21.0   | 482                              |
| 26.5   | 647                              |
| 31.6   | 929                              |
| 36.5   | 1207                             |
| 41.8   | 1548                             |
| 46.5   | 1834                             |
| 52.2   | 2221                             |
| 57.3   | 2612                             |
| 61.7   | 2984                             |
| 66.6   | 3421                             |
| 71.0   | 4432                             |
| 76.7   | 5340                             |
| 79.8   | 6034                             |
| 84.2   | 7365                             |
| 87.2   | 8772                             |
| 92.5   | 11787                            |

Table 5 (Continued)

Test No. 11  
 2.44 inches x 12.44 inches  
 30 inches Deep  
 Density 91.8 lb/ft<sup>3</sup>

| Pressure<br>on Base<br>(lb/in <sup>2</sup> ) | Deflection<br>( <u>inches</u><br>10,000) |
|--|--|
| 1.2  | 0  |
| 4.1  | 372                                      |
| 7.2  | 441                                      |
| 9.9  | 585                                      |
| 12.9   | 815                                      |
| 15.7   | 1097                                     |
| 18.9   | 1005                                     |
| 21.8   | 1997                                     |
| 24.9   | 2537                                     |
| 27.4   | 2955                                     |
| 30.4   | 3614                                     |
| 34.5   | 4370                                     |
| 36.9   | 4823                                     |
| 39.9   | 5585                                     |
| 42.4   | 6150                                     |
| 45.2   | 6891                                     |
| 48.4   | 7857                                     |
| 50.2   | 8987                                     |
| 54.3   | 10437                                    |
| 57.1   | 12943                                    |

Test No. 12  
 2.44 inches x 12.44 inches  
 30 inches Deep  
 Density 82.0 lb/ft<sup>3</sup>

| Pressure<br>on Base<br>(lb/in <sup>2</sup> ) | Deflection<br>( <u>inches</u><br>10,000) |
|--|--|
| 1.2  | 0  |
| 2.4  | 5  |
| 3.6  | 143                                      |
| 4.7  | 484                                      |
| 5.9  | 891                                      |
| 7.0  | 1425                                     |
| 8.3  | 2373                                     |
| 9.3  | 3148                                     |
| 10.6   | 4205                                     |
| 11.9   | 5363                                     |
| 13.0   | 6775                                     |
| 14.3   | 8185                                     |
| 15.4   | 9096                                     |
| 16.5   | 10471                                    |
| 17.9   | 12240                                    |



Table 5 (Continued)

Test 13  
 2.44 inches x 12.44 inches  
 40 inches Deep  
 Density 94.1 lb/ft<sup>3</sup>

| Pressure<br>on Base<br>(lb/in <sup>2</sup> ) | Deflection<br>(inches<br>10,000) |
|--|----------------------------------|
| 1.4  | 0                                |
| 8.6  | 293                              |
| 15.0   | 464                              |
| 21.8   | 805                              |
| 31.0   | 1122                             |
| 37.6   | 1540                             |
| 45.4   | 1957                             |
| 51.9   | 2451                             |
| 59.9   | 2947                             |
| 65.9   | 3561                             |
| 74.3   | 4849                             |
| 81.4   | 6024                             |
| 87.4   | 7899                             |
| 92.3   | 8768                             |
| 93.8   | 10860                            |

Test 14  
 2.44 inches x 12.44 inches  
 40 inches Deep  
 Density 90.7 lb/ft<sup>3</sup>

| Pressure<br>on Base<br>(lb/in <sup>2</sup> ) | Deflection<br>(inches<br>10,000) |
|--|----------------------------------|
| 1.4  | 0                                |
| 5.1  | 257                              |
| 8.8  | 339                              |
| 12.3   | 556                              |
| 15.9   | 1042                             |
| 20.3   | 1744                             |
| 23.6   | 2200                             |
| 27.4   | 2921                             |
| 31.3   | 3562                             |
| 34.3   | 4291                             |
| 38.2   | 5225                             |
| 42.0   | 6202                             |
| 45.0   | 7095                             |
| 49.1   | 8573                             |
| 52.0   | 10870                            |
| 55.0   | 12483                            |

Table 5 (Continued)

Test 15  
 2.44 inches x 12.44 inches  
 40 inches Deep  
 Density 82.0 lb/ft<sup>3</sup>

| Pressure<br>on Base<br>(lb/in <sup>2</sup> ) | Deflection<br>( <u>inches</u><br>10,000) |
|--|--|
| 1.40   | 0  |
| 2.60   | 32                                       |
| 3.60   | 48                                       |
| 4.70   | 141                                      |
| 5.65   | 620                                      |
| 6.90   | 1070                                     |
| 8.00   | 1526                                     |
| 9.10   | 2081                                     |
| 10.25  | 2781                                     |
| 11.50  | 3430                                     |
| 12.40  | 4322                                     |
| 13.40  | 5595                                     |
| 14.70  | 6789                                     |
| 15.60  | 7566                                     |
| 16.70  | 8598                                     |
| 17.90  | 9632                                     |
| 18.55  | 10543                                    |

Test 16  
 2 inches x 12 inches  
 At Surface  
 Density 96.4 lb/ft<sup>3</sup>

| Pressure<br>on Base<br>(lb/in <sup>2</sup> ) | Deflection<br>( <u>inches</u><br>10,000) |
|--|--|
| 3.0  | 145                                      |
| 5.9  | 217                                      |
| 8.9  | 285                                      |
| 11.9   | 360                                      |
| 14.8   | 434                                      |
| 17.5   | 500                                      |
| 20.9   | 586                                      |
| 24.0   | 681                                      |
| 26.6   | 764                                      |
| 28.3   | 870                                      |
| 33.3   | 1043                                     |
| 35.5   | 1132                                     |
| 38.4   | 1303                                     |
| 41.7   | 1560                                     |
| 44.5   | 1848                                     |
| 47.0   | 2185                                     |
| 30.2   | 4770                                     |
| 33.8   | 9102                                     |

Table 5 (Continued)

Test 17  
 2.44 inches x 12.44 inches  
 10 inches Deep  
 Density 95.0 lb/ft<sup>3</sup>

| Pressure<br>on Base<br>(lb/in <sup>2</sup> ) | Deflection<br>( <u>inches</u><br>10,000) |
|--|--|
| 1.0  | 0  |
| 8.3  | 315                                      |
| 15.6   | 383                                      |
| 22.4   | 468                                      |
| 31.0   | 578                                      |
| 36.1   | 680                                      |
| 44.3   | 832                                      |
| 51.5   | 996                                      |
| 58.2   | 1242                                     |
| 66.0   | 1450                                     |
| 72.6   | 1822                                     |
| 80.5   | 2242                                     |
| 87.8   | 2688                                     |
| 95.7   | 3205                                     |
| 102.8  | 3698                                     |
| 110.2  | 4230                                     |
| 118.0  | 4780                                     |
| 123.7  | 5420                                     |
| 121.5  | 7340                                     |
| 117.3  | 8680                                     |
| 120.3  | 12467                                    |

Test 18  
 2.44 inches x 12.44 inches  
 20 inches Deep  
 Density 95.1 lb/ft<sup>3</sup>

| Pressure<br>on Base<br>(lb/in <sup>2</sup> ) | Deflection<br>( <u>inches</u><br>10,000) |
|--|--|
| 1.0  | 0  |
| 11.8   | 133                                      |
| 21.6   | 256                                      |
| 34.1   | 409                                      |
| 44.8   | 580                                      |
| 55.1   | 793                                      |
| 65.9   | 1043                                     |
| 76.1   | 1398                                     |
| 87.7   | 1792                                     |
| 97.0   | 2100                                     |
| 112.0  | 2737                                     |
| 120.0  | 3071                                     |
| 133.0  | 3727                                     |
| 143.2  | 4423                                     |
| 153.8  | 5145                                     |
| 159.8  | 6245                                     |
| 152.0  | 8945                                     |
| 152.0  | 10560                                    |

Table 5 (Continued)

Test 19  
 2.44 inches x 12.44 inches  
 30 inches Deep  
 Density 96.4 lb/ft<sup>3</sup>

| Pressure<br>on Base<br>(lb/in <sup>2</sup> ) | Deflection<br>( <u>inches</u><br>10,000) |
|--|--|
| 1.4  | 0  |
| 14.0   | 204                                      |
| 26.6   | 300                                      |
| 39.3   | 534                                      |
| 52.3   | 757                                      |
| 64.6   | 1022                                     |
| 75.8   | 1402                                     |
| 89.9   | 1803                                     |
| 101.7  | 2135                                     |
| 117.9  | 2684                                     |
| 128.3  | 3093                                     |
| 141.1  | 3680                                     |
| 155.4  | 4443                                     |
| 163.7  | 5294                                     |
| 178.2  | 6432                                     |
| 185.4  | 9151                                     |
| 187.4  | 1558                                     |
| 189.4  | 2554                                     |

Test 20  
 2.44 inches x 12.44 inches  
 40 inches Deep  
 Density 96.5 lb/ft<sup>3</sup>

| Pressure<br>on Base<br>(lb/in <sup>2</sup> ) | Deflection<br>( <u>inches</u><br>10,000) |
|--|--|
| 1.6  | 0  |
| 13.9   | 214                                      |
| 26.0   | 317                                      |
| 38.4   | 474                                      |
| 49.9   | 646                                      |
| 63.0   | 855                                      |
| 76.0   | 1206                                     |
| 87.2   | 1475                                     |
| 99.6   | 1785                                     |
| 111.5  | 2102                                     |
| 124.5  | 2456                                     |
| 136.7  | 2880                                     |
| 149.6  | 3499                                     |
| 164.1  | 4102                                     |
| 172.9  | 4445                                     |
| 177.8  | 5122                                     |
| 193.7  | 7800                                     |
| 197.0  | 8418                                     |
| 201.6  | 10858                                    |

Table 6. Load Settlement Data for Skin Loads

Test No. 7  
 2 inches x 12 inches  
 20 inches Deep  
 Density 93.8 lb/ft<sup>3</sup>

| Average<br>Skin<br>Friction<br>$q_s$<br>(lb/in <sup>2</sup> ) | Deflection<br>(inches<br>10,000) |
|---|----------------------------------|
| 0.054   | 0                                |
| 0.094   | 325                              |
| 0.133   | 738                              |
| 0.168   | 2284                             |
| 0.176   | 3674                             |
| 0.179   | 5866                             |
| 0.188   | 7210                             |
| 0.198   | 8554                             |
| 0.205   | 8958                             |
| 0.214   | 9568                             |
| 0.223   | 9734                             |
| 0.230   | 10219                            |
| 0.238   | 10411                            |
| 0.246   | 10506                            |
| 0.254   | 10664                            |
| 0.271   | 10801                            |

Test No. 8  
 2 inches x 12 inches  
 20 inches Deep  
 Density 90.9 lb/ft<sup>3</sup>

| Average<br>Skin<br>Friction<br>$q_s$<br>(lb/in <sup>2</sup> ) | Deflection<br>(inches<br>10,000) |
|---|----------------------------------|
| 0.053   | 0                                |
| 0.070   | 195                              |
| 0.084   | 286                              |
| 0.100   | 413                              |
| 0.116   | 614                              |
| 0.131   | 932                              |
| 0.147   | 1405                             |
| 0.161   | 3550                             |
| 0.183   | 8739                             |
| 0.197   | 11197                            |
| 0.212   | 12242                            |
| 0.229   | 12912                            |

Table 6 (Continued)

Test No. 9  
 2 inches x 12 inches  
 20 inches Deep  
 Density 82.0 lb/ft<sup>3</sup>

| Average<br>Skin<br>Friction<br>$q_s$<br>(lb/in <sup>2</sup> ) | Deflection<br>(inches<br>10,000) |
|---|----------------------------------|
| 0.054   | 0                                |
| 0.066   | 263                              |
| 0.078   | 313                              |
| 0.090   | 398                              |
| 0.102   | 552                              |
| 0.113   | 827                              |
| 0.124   | 1275                             |
| 0.136   | 2497                             |
| 0.151   | 6010                             |
| 0.164   | 8733                             |
| 0.176   | 9865                             |
| 0.185   | 10457                            |
| 0.210   | 10799                            |

Test No. 10  
 2 inches x 12 inches  
 30 inches Deep  
 Density 94.2 lb/ft<sup>3</sup>

| Average<br>Skin<br>Friction<br>$q_s$<br>(lb/in <sup>2</sup> ) | Deflection<br>(inches<br>10,000) |
|---|----------------------------------|
| 0.043   | 0                                |
| 0.070   | 574                              |
| 0.097   | 605                              |
| 0.124   | 665                              |
| 0.150   | 772                              |
| 0.178   | 854                              |
| 0.204   | 986                              |
| 0.228   | 1214                             |
| 0.261   | 1920                             |
| 0.282   | 2456                             |
| 0.298   | 9740                             |
|   | 10025                            |
|   | 10567                            |

Table 6 (Continued)

Test No. 11  
 2.44 inches x 12.44 inches  
 30 inches Deep  
 Density 91.8 lb/ft<sup>3</sup>

| Average<br>Skin<br>Friction<br>$q_s$<br>(lb/in <sup>2</sup> ) | Deflection<br>(inches<br>10,000) |
|---|----------------------------------|
|---|----------------------------------|

|       |       |
|-------|-------|
| 0.043 | 0     |
| 0.059 | 281   |
| 0.076 | 320   |
| 0.092 | 384   |
| 0.109 | 454   |
| 0.125 | 540   |
| 0.142 | 652   |
| 0.158 | 771   |
| 0.176 | 988   |
| 0.190 | 1430  |
| 0.208 | 1985  |
| 0.224 | 8960  |
| 0.235 | 10887 |

Test No. 12  
 2.44 inches x 12.44 inches  
 30 inches Deep  
 Density 82.0 lb/ft<sup>3</sup>

| Average<br>Skin<br>Friction<br>$q_s$<br>(lb/in <sup>2</sup> ) | Deflection<br>(inches<br>10,000) |
|---|----------------------------------|
|---|----------------------------------|

|       |       |
|-------|-------|
| 0.043 | 0     |
| 0.055 | 26    |
| 0.066 | 56    |
| 0.077 | 173   |
| 0.087 | 214   |
| 0.098 | 305   |
| 0.112 | 371   |
| 0.120 | 518   |
| 0.132 | 692   |
| 0.143 | 1000  |
| 0.153 | 1600  |
| 0.159 | 8900  |
| 0.159 | 10660 |

Table 6 (Continued)

Test No. 13  
 2.44 inches x 12.44 inches  
 40 inches Deep  
 Density 94.1 lb/ft<sup>3</sup>

| Average<br>Skin<br>Friction<br>$q_s$<br>(lb/in <sup>2</sup> ) | Deflection<br>(inches<br>10,000) |
|---|----------------------------------|
|---|----------------------------------|

|       |      |
|-------|------|
| 0.040 | 0    |
| 0.059 | 10   |
| 0.078 | 26   |
| 0.097 | 78   |
| 0.117 | 125  |
| 0.136 | 197  |
| 0.155 | 250  |
| 0.174 | 335  |
| 0.195 | 476  |
| 0.213 | 550  |
| 0.231 | 706  |
| 0.250 | 883  |
| 0.270 | 1140 |
| 0.275 | 7549 |

Test No. 14  
 2.44 inches x 12.44 inches  
 40 inches Deep  
 Density 90.7 lb/ft<sup>3</sup>

| Average<br>Skin<br>Friction<br>$q_s$<br>(lb/in <sup>2</sup> ) | Deflection<br>(inches<br>10,000) |
|---|----------------------------------|
|---|----------------------------------|

|       |      |
|-------|------|
| 0.040 | 0    |
| 0.052 | 140  |
| 0.067 | 148  |
| 0.078 | 170  |
| 0.090 | 224  |
| 0.102 | 275  |
| 0.114 | 325  |
| 0.127 | 381  |
| 0.135 | 443  |
| 0.150 | 509  |
| 0.163 | 590  |
| 0.175 | 694  |
| 0.187 | 830  |
| 0.198 | 1007 |
| 0.210 | 1356 |
| 0.235 | 8810 |



Table 6 (Continued)

Test No. 15  
 2.44 inches x 12.44 inches  
 40 inches Deep  
 Density 82.0 lb/ft<sup>3</sup>

| Average<br>Skin<br>Friction<br>$q_s$<br>(lb/in <sup>2</sup> ) | Deflection<br>( <u>inches</u><br>10,000) |
|---|--|
|---|--|

|       |      |
|-------|------|
| 0.041 | 0    |
| 0.053 | 244  |
| 0.067 | 283  |
| 0.079 | 385  |
| 0.092 | 466  |
| 0.103 | 552  |
| 0.115 | 651  |
| 0.126 | 740  |
| 0.140 | 897  |
| 0.153 | 1009 |
| 0.167 | 1105 |
| 0.177 | 1358 |
| 0.188 | 1715 |
| 0.206 | 5690 |
| 0.212 | 8763 |

Test No. 18  
 2.44 inches x 12.44 inches  
 20 inches Deep  
 Density 95.1 lb/ft<sup>3</sup>

| Average<br>Skin<br>Friction<br>$q_s$<br>(lb/in <sup>2</sup> ) | Deflection<br>( <u>inches</u><br>10,000) |
|---|--|
|---|--|

|       |      |
|-------|------|
| 0.051 | 0    |
| 0.072 | 46   |
| 0.086 | 83   |
| 0.106 | 91   |
| 0.120 | 100  |
| 0.138 | 112  |
| 0.155 | 141  |
| 0.170 | 170  |
| 0.187 | 203  |
| 0.204 | 246  |
| 0.221 | 302  |
| 0.238 | 437  |
| 0.255 | 565  |
| 0.272 | 725  |
| 0.281 | 1092 |
| 0.299 | 3602 |
| 0.298 | 8325 |

Table 6 (Continued)

Test No. 19  
 2.44 inches x 12.44 inches  
 30 inches Deep  
 Density 96.4 lb/ft<sup>3</sup>

| Average<br>Skin<br>Friction<br>$q_s$<br>(lb/in <sup>2</sup> ) | Deflection<br>(inches<br>10,000) |
|---|----------------------------------|
|---|----------------------------------|

|       |       |
|-------|-------|
| 0.042 | 0     |
| 0.072 | 34    |
| 0.097 | 59    |
| 0.124 | 114   |
| 0.152 | 178   |
| 0.179 | 310   |
| 0.207 | 518   |
| 0.235 | 778   |
| 0.264 | 838   |
| 0.284 | 872   |
| 0.318 | 939   |
| 0.350 | 996   |
| 0.368 | 1048  |
| 0.398 | 1145  |
| 0.430 | 1310  |
| 0.456 | 1510  |
| 0.484 | 2304  |
| 0.515 | 8112  |
| 0.454 | 9936  |
| 0.476 | 10425 |

Test No. 19\*  
 2.44 inches x 12.44 inches  
 30 inches Deep  
 Density 96.4 lb/ft<sup>3</sup>

| Average<br>Skin<br>Friction<br>$q_s$<br>(lb/in <sup>2</sup> ) | Deflection<br>(inches<br>10,000) |
|---|----------------------------------|
|---|----------------------------------|

|        |      |
|--------|------|
| +0.042 | 0    |
| +0.024 | 3    |
| +0.007 | 1    |
| -0.008 | 3    |
| -0.058 | 4    |
| -0.075 | 29   |
| -0.092 | 53   |
| -0.109 | 81   |
| -0.126 | 114  |
| -0.145 | 146  |
| -0.160 | 378  |
| -0.152 | 7267 |
| -0.138 | 8644 |

\* Pull skin after pushing

Table 6 (Continued)

Test No. 20  
 2.44 inches x 12.44 inches  
 40 inches Deep  
 Density 96.5 lb/ft<sup>3</sup>

| Average<br>Skin<br>Friction<br>$q_s$<br>(lb/in <sup>2</sup> ) | Deflection<br>(inches<br>10,000) |
|---|----------------------------------|
|---|----------------------------------|

|       |      |
|-------|------|
| 0.041 | 0    |
| 0.078 | 239  |
| 0.101 | 258  |
| 0.140 | 266  |
| 0.174 | 283  |
| 0.208 | 298  |
| 0.241 | 316  |
| 0.272 | 335  |
| 0.306 | 355  |
| 0.339 | 379  |
| 0.368 | 409  |
| 0.406 | 456  |
| 0.437 | 497  |
| 0.472 | 550  |
| 0.513 | 621  |
| 0.538 | 674  |
| 0.570 | 775  |
| 0.596 | 914  |
| 0.631 | 1079 |
| 0.673 | 1715 |
| 0.711 | 2835 |
| 0.744 | 4287 |
| 0.754 | 6378 |
| 0.752 | 8646 |

Test No. 20\*  
 2.44 inches x 12.44 inches  
 40 inches Deep  
 Density 96.5 lb/ft<sup>3</sup>

| Average<br>Skin<br>Friction<br>$q_s$<br>(lb/in <sup>2</sup> ) | Deflection<br>(inches<br>10,000) |
|---|----------------------------------|
|---|----------------------------------|

|        |      |
|--------|------|
| +0.040 | 0    |
| +0.020 | 0    |
| -0.008 | 8    |
| -0.025 | 19   |
| -0.041 | 32   |
| -0.068 | 59   |
| -0.081 | 86   |
| -0.153 | 215  |
| -0.162 | 234  |
| -0.182 | 285  |
| -0.202 | 371  |
| -0.216 | 8728 |

\* Pull skin after pushing

Table 6 (Continued)

Test No. 20\*\*  
 2.44 inches x 12.44 inches  
 40 inches Deep  
 Density 96.5 lb/ft<sup>3</sup>

| Average<br>Skin<br>Friction<br>$q_s$<br>(lb/in <sup>2</sup> ) | Deflection<br>( <u>inches</u><br>10,000) |
|---|--|
| 0.040   | 0  |
| 0.073   | 410                                      |
| 0.103   | 482                                      |
| 0.136   | 608                                      |
| 0.169   | 786                                      |
| 0.205   | 1090                                     |
| 0.233   | 1490                                     |
| 0.266   | 2132                                     |
| 0.300   | 3595                                     |
| 0.334   | 5747                                     |
| 0.360   | 8321                                     |

\*\* Push skin again after pulling

## BIBLIOGRAPHY

1. Terzaghi, Karl, Theoretical Soil Mechanics, 1st ed. New York: John Wiley and Sons, Inc., 1943, p. 124.
2. De Beer, E. E., and A. B. Vesic, "Etude experimentale de la capacité portante du sable sous des fondations directes établies en surface," Annales des Travaux Publics de Belgique, 3, (1958), pp. 50-51.
3. Skempton, A. W., and A. A. Yassin, "Theorie de la force portante des pieux dans le sable," Annales de l'Institut Technique du Batiment et des Travaux Publics, 7, 8 and 9 (1952), p. 286.
4. Ibid., p. 287.
5. Fausold, H. M., Model Studies of Pile Bearing Capacity Relationships in a Cohesive Soil, Unpublished Master's Thesis, Georgia Institute of Technology, 1960.
6. Chaplin, T. K., "Compressibility of Sands and Settlement of Model Footings and Piles in Sand," Proceedings Fifth International Conference on Soil Mechanics and Foundation Engineering, 2 (1961), p. 33.
7. Mogami, T., and K. Kubo, "The Behavior of Soils During Vibration," Proceedings Third International Conference on Soil Mechanics and Foundation Engineering, 1 (1953), p. 155.
8. De Beer and Vesic, op. cit., p. 38.
9. De Beer and Vesic, op. cit., p. 5.
10. Hansen, B., "The Bearing Capacity of Sand, Tested by Loading Circular Plates," Proceedings Fifth International Conference on Soil Mechanics and Foundation Engineering, 1 (1961), p. 659.
11. Chen, Liang-Sheng, "An Investigation of Stress-Strain and Strength Characteristics of Cohesionless Soils by Triaxial Compression Tests," Proceedings Second International Conference on Soil Mechanics and Foundation Engineering, 5 (1948), p. 40.
12. Caquot, A., and J. Kérisel, "Sur le terme de surface dans le calcul des fondations en milieu pulvérulent," Proceedings Third International Conference on Soil Mechanics and Foundation Engineering, 1 (1953), p. 33.
13. Meyerhof, G. G., "The Ultimate Bearing Capacity of Foundations," Géotechnique, 2 (1951), p. 306.

14. Hansen, J. B., "Simple Statical Computation of Permissible Pile Loads," Christiani and Nielson Post, 13 (1951), p. 14.
15. Kérisel, J., "Fondations profondes en milieux sableux: variation de la force portante limite en fonction de la densité, de la profondeur, du diamètre et de la vitesse d'enfoncement," Proceedings Fifth International Conference on Soil Mechanics and Foundation Engineering, 2 (1961), p. 73.
16. Terzaghi, Karl, and Peck, R. B., Soil Mechanics in Engineering Practice, New York: John Wiley and Sons, Inc., 1948, p. 140.
17. Tschebotarioff, Gregory P., Soil Mechanics, Foundations and Earth Structures, New York: McGraw-Hill Book Company, Inc., 1953, p. 258.